

THESIS WORK FOR DUAL MASTER'S DEGREE

ITBA - Mag. in Energy and Environment

KIT - MSc. in Mechanical Engineering

Transient Simulation and Validation of a Condenser for a Supercritical Organic Rankine Cycle

Mariano Javier Fossati

Mechanical Engineer
Universidad Tecnológica Nacional

Tutor

Prof. Dr. Ing. Thomas Schulenberg, KIT, ITES

Co-Tutor

Dipl.-Ing. Hans-Joachim Wiemer

Examiners

Prof. Dr. Ing. Thomas Schulenberg (ITES/KIT)

Prof. Dr. Ing. Andreas Class (ITES/KIT)

Dr. Ing. Cecilia Smoglie (ITBA)

Karlsruhe
10/05/2020

Statement

Ich versichere wahrheitsgemäß, die Arbeit selbstständig verfasst, alle benutzten Hilfsmittel vollständig und genau angegeben und alles kenntlich gemacht zu haben, was aus Arbeiten anderer unverändert oder mit Abänderungen entnommen wurde sowie die Satzung des KIT zur Sicherung guter wissenschaftlicher Praxis in der jeweils gültigen Fassung beachtet zu haben.

Karlsruhe

Mariano Javier Fossati

Abstract

This work contains a development of a fluid and thermodynamic model for a condenser with horizontal pipes and plain fins and its application for a dynamic model in Simulink with the purpose of studying transient regimes in the condenser on a mobile research geothermal power plant located at Campus Nord KIT called MoNiKa. During the model design, different methods and correlations for the prediction of the pressure loss and the heat transfer were tested and the results for the final version of the model are presented and compared with measured values for validation. The validation took place in two different steps, the first one for a first approach with different stationary points, and the second with transient data from test runs from MoNiKa.

The dynamic model was built in Simulink with different blocks with Matlab code based. All the physical properties of the fluids were extracted from the REFPROP, which is a data base from the National Institute of Standards and Technology (NIST). All the properties needed for the simulation are first migrated to a data base in Matlab and then used by the program as dynamic lookup tables, this help to improve the time response of the simulation.

Parameter as pressure, enthalpy and temperature were compared for the validation and analysis of the predicted values, where a good approximation of the reality is shown. In the specific area of the pressure loss, better sensors are needed for further analysis. This first model for a transient condenser is a good ground base but it need to be upgrade for a humid air scenario, which is one of the features of the installed condenser.

Resumen

Este trabajo contiene el desarrollo de un modelo tanto, fluidodinámico como termodinámico, para un condensador con tubos horizontales y aletas planas, además de su aplicación para un modelo dinámico en Simulink con el propósito de estudiar los regímenes transitorios del condensador en una planta de investigación geotérmica móvil ubicada en Campus Nord KIT llamada MoNiKa. Durante el diseño del modelo, se probaron diferentes métodos y correlaciones para la predicción de la pérdida de presión y la transferencia de calor. Los resultados de la versión final, son presentados comparados con valores medidos para su validación. La validación se llevó a cabo en dos pasos, el primero se trata de una primera aproximación con diferentes puntos estacionarios, y el segundo con datos transitorios de las pruebas del MoNiKa.

El modelo dinámico se construyó en Simulink con diferentes bloques basados en el código Matlab. Todas las propiedades físicas de los fluidos fueron extraídas del REFPROP, que es una base de datos del Instituto Nacional de Estándares y Tecnología (NIST). Todas las propiedades necesarias para la simulación se migran primero a una base de datos en Matlab y luego son utilizadas por el programa como tablas de búsqueda dinámica, esto ayuda a mejorar la respuesta temporal de la simulación.

Parámetros como presión, entalpía y temperatura fueron comparados para la validación y el análisis de los valores predichos, donde se muestra una buena aproximación de la realidad. En el caso específico de la pérdida de presión, mejores sensores son necesarios para lograr un análisis conclusivo. Este primer modelo para un condensador transitorio es un buen modelo base, pero necesita ser mejorado, por ejemplo, para un escenario de aire húmedo, que es una de las características del condensador instalado.

Zusammenfassung

Diese Arbeit beinhaltet die Entwicklung eines flüssigkeits- und thermodynamischen Modells für einen Kondensator mit horizontalen Rohren und glatten Lamellen und seine Anwendung für ein dynamisches Modell in Simulink mit dem Ziel, instationäre Regime im Kondensator eines mobilen geothermischen Forschungs-Kraftwerks am Campus Nord des KIT namens MoNiKa zu untersuchen. Während des Modelldesigns wurden verschiedene Methoden und Korrelationen für die Vorhersage des Druckverlusts und der Wärmeübertragung getestet. Die Ergebnisse für die endgültige Version des Modells werden präsentiert und zur Validierung mit gemessenen Werten verglichen. Die Validierung erfolgte in zwei verschiedenen Schritten, der erste für einen ersten Ansatz mit verschiedenen stationären Punkten und der zweite mit instationären Daten aus Testläufen von MoNiKa.

Das dynamische Modell wurde in Simulink mit verschiedenen Blöcken auf der Basis von Matlab-Code aufgebaut. Alle physikalischen Eigenschaften der Fluide wurden aus dem REFPROP, einer Datenbank des National Institute of Standards and Technology (NIST), extrahiert. Alle für die Simulation erforderlichen Eigenschaften werden zunächst in eine Datenbank in Matlab migriert und dann vom Programm als dynamische Lookup-Tabellen verwendet, wodurch das Zeitverhalten der Simulation verbessert wird.

Parameter wie Druck, Enthalpie und Temperatur wurden für die Validierung und Analyse der vorhergesagten Werte verglichen, wobei eine gute Annäherung an die Realität gezeigt wird. In dem speziellen Bereich des Druckverlustes werden für die weitere Analyse bessere Sensoren benötigt. Dieses erste Modell für einen instationären Kondensator ist eine gute Basis, aber es muss für ein Feuchtluftzenario nachgerüstet werden, was eines der Merkmale des installierten Kondensators ist.

Table of contents

Statement	I
Abstract	II
Resumen	III
Zusammenfassung	IV
Table of contents	V
List of symbols	VII
1 Introduction	1
2 Basic principles	3
2.1 Organic Rankine Cycle	3
2.2 Condenser	4
2.3 Basic equations for fluid dynamics	6
2.4 Void fraction	10
2.5 Pressure Loss	11
2.6 Heat Transfer	14
2.6.1 Outer heat transfer coefficient – Air side	15
2.6.2 Surface efficiency	18
2.6.3 Inner heat transfer coefficient – Propane side	18
3 Programming and simulation	22
3.1 REFPROP	22
3.2 Simulink	22
3.3 Code beginning	22
3.4 Two Phase fluid tables	24
3.5 Functional flow of the Program	26
3.6 First simulations	31
4 Results and Validation	33
4.1 Data input	33
4.2 Verification	37
4.3 Stationary validation	39
4.3.1 Pressure validation	39
4.3.2 Temperature and enthalpy validation	40
4.4 Transient validation	43

5	Summary and Conclusions	48
6	References	51
7	Appendix.....	53
7.1	List of tables.....	53
7.2	List of figures	54

List of symbols

Symbols

A	Area	$[m^2]$
A_o	Outer area per unit length	$[m]$
A_{bo}	Bare tube outer area per unit length	$[m]$
A_{fin}	Fin area per unit length	$[m]$
A_{min}	Minimum flow area per unit length	$[m]$
d	Diameter	$[m]$
d_h	Hydraulic diameter	$[m]$
e	Internal energy	$[J/kg]$
f	Friction factor	$[-]$
g	Gravity constant	$[m/s^2]$
G	Mass flux	$[Kg/(s.m^2)]$
h	Enthalpy	$[J/kg]$
k	Overall heat transfer coefficient	$[W/(m^2.K)]$
K	Pressure loss coefficient	$[-]$
\dot{M}	Mass flow	$[kg/s]$
N	Number of rows	$[-]$
n	Number of tubes per row	$[-]$
P	Perimeter	$[m]$
p	Pressure	$[Pa]$
Q	Heat	$[J]$
\dot{Q}_s	Source heat rate per kg	$[W/kg]$
\dot{Q}	Heat rate	$[W]$
\dot{q}_w	Wall heat flux	$[W/m^2]$
T	Temperature	$[K]$
t_{fin}	Thickness of the fin	$[m]$
u_d	Diagonal length between tube	$[m]$
u_l	Longitudinal length between tube	$[m]$
u_t	Transversal length between tube	$[m]$
w	Velocity	$[m/s]$

x	Quality	[-]
z_{finm}	Density of fins per meter	[1/m]
α	Heat transfer coefficient	[W/(m ² .K)]
Γ	Mass transfer of the phase by evaporation or condensation	[kg/(m.s)]
Δp	Pressure loss	[Pa]
Δz	Length of a cell	[m]
ε	Void fraction	[-]
ε_h	Homogeneous Void fraction	[-]
ε_{ra}	Void fraction drift flux model of Rouhani and Axelsson	[-]
η	Relative roughness	[-]
η_o	Surface efficiency	[-]
κ	Absolute roughness	[m]
λ	Thermal conductivity	[W/(m.K)]
ξ	Form loss coefficient	[-]
μ	Dynamic viscosity	[kg/(m.s)]
ρ	Density	[kg/m ³]
σ	Surface tension	[N/m]
τ	Shear stress	[Pa]
Φ	Two phase coefficient	[-]

Dimensionless numbers

Re	Reynolds Number
Nu	Nusselt Number
Pr	Prandtl Number
We	Weber Number
Fr	Froude Number
j	Colburn j factor

Subscript

j	Liquid or Gas
L	Liquid
G	Gas

M	Mixture
I	Impulse
E	Energy

Abbreviations

MoNiKa	Modularer Niedertemperaturkreislauf Karlsruhe
ORC	Organic Rankine Cycle
REFPROP	Reference Fluid Properties

1 Introduction

In the last years, the world has become increasingly alarmed and active about the consequences of global climate change. Thus, the use of renewable, low CO₂ supplier source of energy, more specifically electric power, are in great demand. This demand is increasing as a response of the world governments and the energy companies to a claim of the scientific community and the consumers to try to reduce the production of greenhouse gases. Geothermal energy, in addition to bioenergy, hydropower, solar energy, wind energy and others, is an option to this increasing demand.

Geothermal energy is the use of the thermal energy produced and stored beneath the earth's surface, and it can be found anywhere in the world, but the high temperature energy that is needed to electric generation is only found in a limited places. If one were to drill a well in the surface of the earth and measure the temperature as function of the depth, a properly constant of 3 K for each 100 m will be found [20]. The temperature of the thermal water vary to the place where is originated, and there exist many places with low-temperature range between 100 °C and 200 °C. With the objective of harvest this low-temperature energy, thermal cycles with organic working fluids are used. This kind of processes are called Organic Rankine Cycle.

The Institute of Thermal Energy Technology and Safety (ITES) install at the site of the Karlsruhe Institute of Technology Campus North (KIT-CN), a mobile research geothermal power plant, MoNiKa (modular low-temperature circuit Karlsruhe). MoNiKa is a compact small power plant with a thermal output of 1000 kW, that has as objective the thermodynamically and economically optimization of both, the individual components and the cycle as a whole. The results of the research carried out on MoNiKa contribute to increasing the efficiency of power generation from low-enthalpy geothermal sources. Therefore, the study and optimization of a cooling system for the power plant process is particularly important.

MoNiKa is operating as a supercritical process with propane as the working medium, since the investigation with supercritical circuits achieved higher net power outputs than subcritical ones, given by the fact that the energy can be extracted from the thermal water at lower temperatures since no isothermal evaporation takes place [28].

Since MoNiKa is a mobile research geothermal power plant, the condenser was designed with air as a cooling fluid. The hybrid cooling towers can work with dry or wet air depending the necessities of the plant. The efficiency of the plant is important and the power consumption of the fans installed on the cooling tower is significant, therefore is important to study and optimize the condenser system.

The aim of this work is to design and perform a transient program and model capable of perform simulations of the condenser for different load points with the program Simulink, the measurement of experimental data of the transient load points at MoNiKa cycle and its later analysis, validation, interpretation and comparison of the measured data with the predicted one. For the analysis, the identification of the sensibility of the individual parameters would be helpful to be done.

For all this tests, the cycle will be performing in by-pass with a throttling valve acting instead of the turbine, this is meant to avoid any complexity to the basic data for simulation and validation, and to avoid any mechanical problems that can emerge with the installation of new and complex equipment as the turbine is.

A research to obtain the main fundamentals for the development of the physic model is needed in order to predict the real condenser already installed with the best accuracy possible. As a request for the scope of the master thesis, the development of the model will be in Simulink [25] and all properties of fluids used in this thesis investigation where provided by the software REFPROP [16].

For all the data needed in this study for validation and comparison, different test runs on MoNiKa are needed, in which I will be present with the team in charge of collecting this data.

2 Basic principles

2.1 Organic Rankine Cycle

The Rankine cycle is widely used in process of power generation through the conversion of thermal energy. The typical heat sources for this process are combustion of fossil fuels and nuclear fission and usually uses water as a primary fluid. Other less used sources are the geothermal energy, solar energy and biomass, however those are low enthalpy sources and the Rankine process is not suitable in this case, because it needs high pressures that are associated to high evaporation temperatures. Instead of water, organic fluids are used as a working medium in the Organic Rankine Cycle (ORC). Compared to water, these are characterized by lower evaporation temperatures and pressures. The ideal Rankine cycle is composed of these four steps:

1. Isentropic compression by work input in the pump.
2. Isobaric heat input in the heat exchanger.
3. Isentropic expansion by release of work in the turbine.
4. Isobaric heat release in the condenser

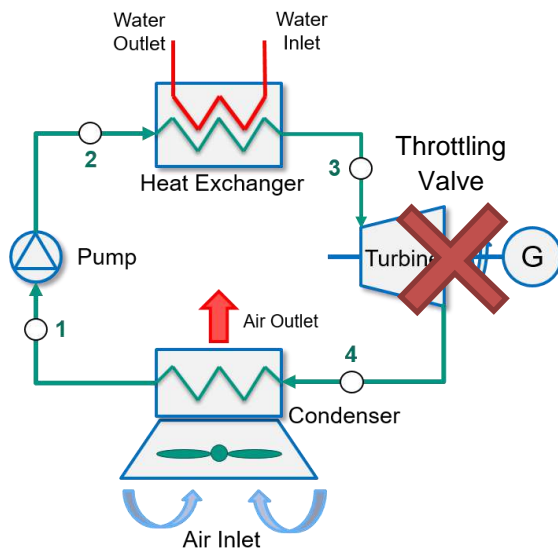


Figure 2.1 Diagram of the Rankine Cycle

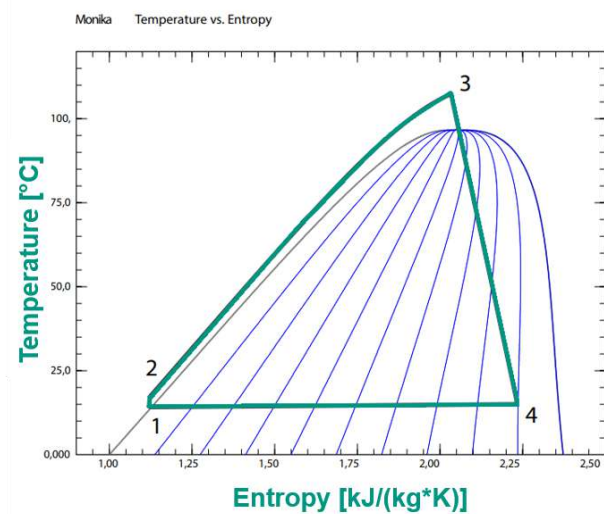


Figure 2.2 T-S Diagram of MoNiKa ORC at full load

Nevertheless, those four state changes are not possible to achieve since they are ideal. In a real case, the pump and the turbine have isentropic efficiencies given by mechanical and fluid losses. Also the existence of pressure losses on the heat exchanger and the condenser leads to a further difference with the ideal case.

Figure 2.1 shows a simple diagram with all four processes on a Rankine cycle. The first process is taking place in a piston pump, which compresses the primary fluid. In second, the hot water provided heat to the propane. Next, the primary fluid expands until it gets a small condensation in the turbine, always watching to not get damage in the turbine blades, and transfer work to the generator. And

finally, the propane gets a full condensation by dissipating heat in the condenser. As it was mentioned in the introduction, in our case of study the turbine is in by-pass replaced by a throttling valve.

In Figure 2.2 it is represented a T-S diagram of the MoNiKa cycle at full load. The points marked are coincident with the ones discussed. The pressure from 2 to 3 is always supercritical, and in point 3 pressure and temperature are supercritical. In the case of propane this values are: 4.25 MPa and 369.89 K (96.74 °C).

The reason for using a supercritical cycle is because a higher net output can be achieved than with a subcritical fluid. This fact and the reasons for using propane as a primary fluid in MoNiKa are explained in the investigation of *Christian Vetter et al.* [28].

2.2 Condenser

For this study, all the geometrical and material properties of the condenser already installed in MoNiKa are used. The primary fluid of the condenser, and of the whole cycle, is propane. The secondary fluid is air. The properties of humid air are not taken in account in this study. In Figure 2.3 is shown that the condenser is assembled with 3 fans, each one is a set of impeller plus the diffusor, a heat exchange area in both sides, water sprays, and the structure holding all the previous parts.

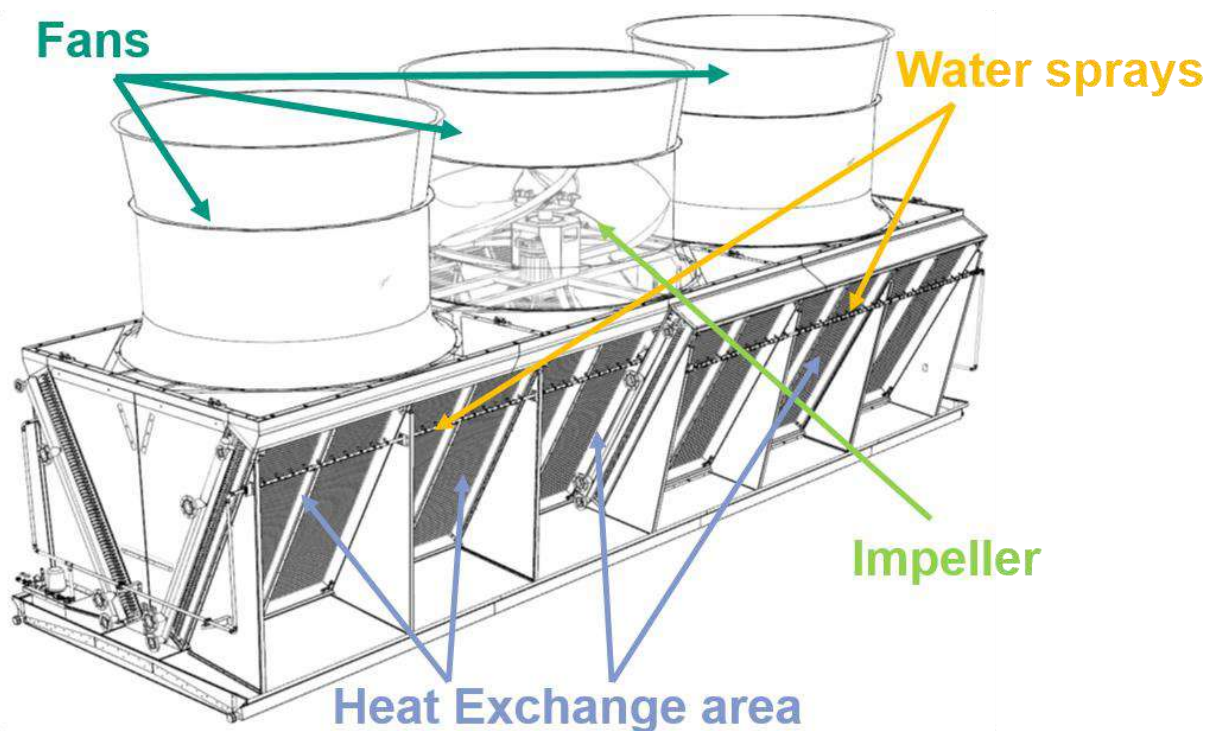


Figure 2.3 MoNiKa condensers layout [12]

The fans are induced draft type, the impellers diameter is about 2475 mm and they rotation design speed is 322 RPM. The estimated air flow by the manufacturer for that speed is 44 m³/s and the fan shaft power is 9.9 kW [29].

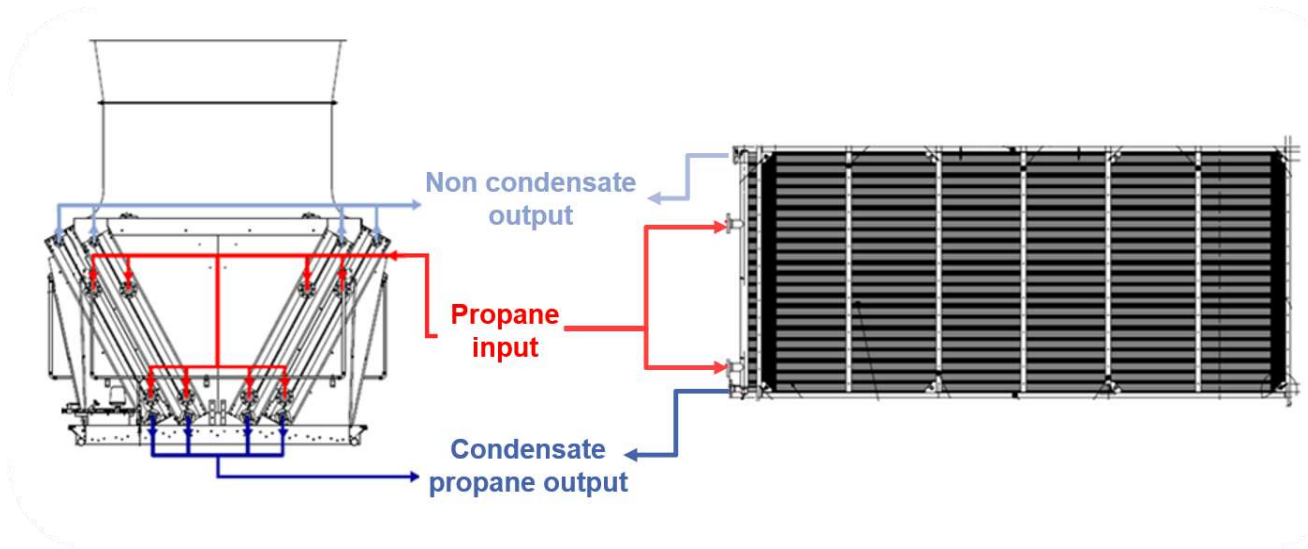


Figure 2.4 Condenser heat exchange module [12]

The heat exchange areas are built in a symmetrical way at both sides of the condenser as Figure 2.4 shows on the left side. Each side has 2 separate modules of heat exchange area. Each of these modules (see Figure 2.4 on the right), is integrated by a vertical tube with two propane entrances, these tube then distributes the propane in 69 smaller horizontal tubes of 11 mm internal diameter and a thickness of 0.5 mm. These are the principal components of the condenser, each tube has a length of around 20.5 m but is divided in different rows, this means that the tube (as it is represented on the right side of the Figure 2.4) goes from left to right, turns and comes back in the same direction, then again repeats the same trajectory giving a number of 4 rows. At last, a bigger vertical tube, similar to the one on the entrance, collects the propane from all 69 horizontal tubes and exits the condenser in two ways, one as pure fluid on the bottom, and another one at the top as gas. The propane is mostly full condensate, so gas absent at the exit of the top, but this exit helps to separate other non-condensable fluids from the propane and purge them from the cycle if it is necessary.

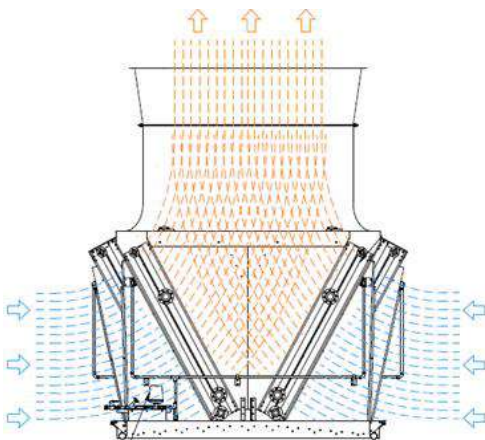


Figure 2.5 Air flow path in the condenser [12]

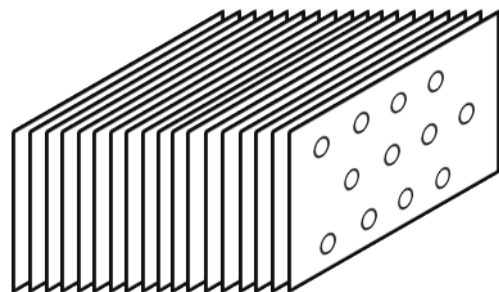


Figure 2.6 Fin stack and tube bundle arrangement

All the horizontal tubes are running through a stack of flat plain rectangular fins with a thickness of 0.15 mm. A representation of the arrangement of the fins is shown in Figure 2.5, but instead of 3

rows, the condenser has 69. It also shows the staggered arrangement of the 4 columns of the tubes. Different types of stainless steels are used in all the heat exchange module, such as AISI 304, AISI 316L and AISI 303, the only exception are the fins. These are made of an aluminum alloy with a special coating.

Figure 2.6 exhibits the flow path of the air on the condenser, how the cold air of the ambient is pulled by the fan, going through the finned tube bundle while heating up and losing some pressure, and at last exiting the fan through the diffuser. It is important to highlight that primary and secondary fluids work in cross flow in this particular condenser.

2.3 Basic equations for fluid dynamics

The first approach for the study was to set the ground for the physic properties of the working fluid. The design of the condenser and the different test made in MoNiKa, set the inlet of propane to the condenser as a two phase fluid, with a quality x depending on the turbine or the throttling valve. Also the outlet of the condenser is set by design to be as a saturated liquid or a little subcooled liquid; the tests prove that the real condenser is working at the outlet in the subcooled area very close to the saturated liquid. This indicates that almost all heat is exchanged with the propane as a two phase fluid.

In this study, 3 governing equations are proposed: mass balance, momentum balance and energy balance, which are differential formulas based on the Reynolds transport theorem. This task was guided by Prof. Dr. Thomas Schulenberg and material of the Two phase flow Lecture [18]. Equation (2.1) displays the mass balance for both phases. The subscript j indicates the type of phase, could it be liquid (denoted in all this work with the subscript L) or gas (denoted in all this work with the subscript G).

$$\frac{\partial}{\partial t} A_j \rho_j + \frac{\partial}{\partial z} \dot{M}_j = \Gamma_j \quad (2.1)$$

A is the total area of the fluid or phase of the fluid, ρ denotes the density and \dot{M} the mass flow. Γ_j is the mass transfer of the phase by evaporation or condensation per length unit. Is necessary to define the quality of the fluid as the ratio between the gas mass flow and the total mass flow of the fluid, equation (2.2). In a similar way, the void or volume ratio, is defined as the ratio between the volume occupied by the gas and the total volume of the fluid. Inside of a tube which is going to be discretized in a longitudinal way, the definition is given by the ratio of the areas between gas and total fluid in each length differential, equation (2.3).

$$x = \frac{\dot{M}_G}{\dot{M}}; \quad 1 - x = \frac{\dot{M}_L}{\dot{M}} \quad (2.2)$$

$$\varepsilon = \frac{A_G}{A}; \quad 1 - \varepsilon = \frac{A_L}{A} \quad (2.3)$$

With these definitions, it is possible to present the balance for both phases like it is shown in equations (2.4) and (2.5). With the assumption that both phases are in thermodynamic equilibrium, but may be in a mechanical non-equilibrium, it is possible to get the equation (2.6) by adding the two previous ones. I assume a drift flux model in which both phases travel at different velocities, in contrast to the homogeneous model that considers both phases traveling with the same velocity. The slip ratio is the ratio between the velocities of the gas and the liquid, and it is equals to 1 for the homogenous model. The slip ratio usually has an important role in the fluid and thermal dynamics, which is the reason of considering the drift flux model.

$$\frac{\partial}{\partial t} (1 - \varepsilon) \rho_L + \frac{1}{A} \frac{\partial}{\partial z} (1 - x) \dot{M} = -\frac{\Gamma_L}{A} \quad (2.4)$$

$$\frac{\partial}{\partial t} \varepsilon \rho_G + \frac{1}{A} \frac{\partial}{\partial z} x \dot{M} = \frac{\Gamma_G}{A} \quad (2.5)$$

$$\frac{\partial}{\partial t} \rho_M + \frac{1}{A} \frac{\partial}{\partial z} \dot{M} = 0 \quad (2.6)$$

The first term of the equation (2.6) is the time dependent term, e.g. due to accumulation or disappearance of mass within the control volume. The second one is the net flow through the surface of the control volume. In this particular case of study, I am going to neglect the first term, since I am not considering quick changes in the density or the pressure, that are given usually by high velocity events like cavitation. This will lead to a quasi-steady-state approach, in which the slow transients of energy are consider only. It is not the objective of the study to analyze flow instability regimes in the condenser. As a resume of this balance, I can say that the inlet mass flow of the condenser is equals to the outlet at any time.

The second balance to be made is the momentum. In analogous way and under the same assumptions, the equation (2.7) and (2.8) presents the momentum balance for both phases, and the equation (2.9) is the result of adding the previous two.

$$\frac{\partial}{\partial t} \dot{M}_G + \frac{\partial}{\partial z} \frac{\dot{M}_G^2}{A_G \rho_G} = -A_G \frac{\partial}{\partial z} p_G + P_i \tau_{iG} - P_G \tau_{wG} - A g \rho_G \sin \varphi + \Gamma_G w_i \quad (2.7)$$

$$\frac{\partial}{\partial t} \dot{M}_L + \frac{\partial}{\partial z} \frac{\dot{M}_L^2}{A_L \rho_L} = -A_L \frac{\partial}{\partial z} p_L + P_i \tau_{iL} - P_L \tau_{wL} - A g \rho_L \sin \varphi + \Gamma_L w_i \quad (2.8)$$

$$\frac{\partial}{\partial t} \dot{M} + \frac{\partial}{\partial z} \frac{\dot{M}^2}{A \rho_I} = -A \frac{\partial p}{\partial z} - P_w \tau_{wM} - A g \rho_M \sin \varphi \quad (2.9)$$

I assume that the pressure in the whole fluid and so in both phases is the same. The first term in this balance is the time dependent term, and is neglected as well since the mass balance does not consider quick changes on time. The second term is the net flow of pressure through the surface of the control volume. On the other side of the equation, there is a sum of external forces, the first term in all equations is given by the pressure force. τ_{iG} and τ_{iL} represents the interfacial shear stress, and the sum of both is zero. $P_w \tau_{wM}$ is the friction force of the mixture against the wall of the tube. Then there is the gravity term, and finally $\Gamma_L w_i$ and $\Gamma_G w_i$ are Momentum transfer due to mass transfer with interface velocity w_i . In the worst case scenario, where all the tubes are filled with liquid propane, the gravity term has a value of 10 kPa, for the almost 2 m difference between the lowest and the highest tube in the modules. This difference in hydrostatical pressure is neglected, since the model, simulates only one tube under the assumption that the mass flow is equally distributed in all 69 tubes.

The values without subscript like the pressure or the mass flow, refer to the total value for the mixture; the same applies for the area A, which is the total inner area.

The energy balance for both phases is displayed in equations (2.11) and (2.12), and for the mixture in equation (2.13). In this case, the balance is a function of the enthalpy:

$$h = e + \frac{p}{\rho} \quad (2.10)$$

Where e is the internal energy of the fluid and p/ρ represents the flow energy of the fluid. As in all balances presented, the first term of the energy balance is the time dependent term. In this case, is very important because it will show a transient effect of the condenser. The second one is the net energy going through the surface of the control volume. On the other side of the equation, the first term comes from the time dependent enthalpy term and represents the transient pump work but, in this study, there is no variation of pressure considered over time.

$$\begin{aligned} A \frac{\partial}{\partial t} \varepsilon \rho_G h_G + \frac{\partial}{\partial z} x \dot{M} h_G \\ = A \frac{\partial}{\partial t} \varepsilon p + P_G \dot{q}_{wG} + P_i \dot{q}_{iG} + A \varepsilon \rho_G \dot{Q}_s + \Gamma_G \Delta h_{LG} + x \dot{M} g \sin \varphi \end{aligned} \quad (2.11)$$

$$\begin{aligned} A \frac{\partial}{\partial t} (1 - \varepsilon) \rho_L h_L + \frac{\partial}{\partial z} (1 - x) \dot{M} h_L \\ = A \frac{\partial}{\partial t} (1 - \varepsilon) p + (P - P_G) \dot{q}_{wL} + P_i \dot{q}_{iL} + A (1 - \varepsilon) \rho_L \dot{Q}_s + \Gamma_L \Delta h_{LG} + (1 - x) \dot{M} g \sin \varphi \end{aligned} \quad (2.12)$$

$$A \frac{\partial}{\partial t} \rho_M h + \frac{\partial}{\partial z} \dot{M} \left(h + \frac{\dot{M}^2}{2 \rho_E^2 A^2} \right) = A \frac{\partial p}{\partial t} + P_H \dot{q}_w + A \rho_M \dot{Q}_s + \dot{M} g \sin \varphi \quad (2.13)$$

\dot{q}_{iG} and \dot{q}_{iL} are the heat flux of superheated or subcooled phases to the interface; it was assumed before that both phases are in thermodynamic equilibrium, so the sum of both is zero. \dot{q}_w is the heat flux transferred between primary and secondary fluids through the wall of the tubes and its fins. P denotes the perimeter where the heat transfer happens. \dot{Q}_s represents a heat source inside the control volume, which is nonexistent in this case. The last term is the representation of the potential energy. The sum in (2.14) is the energy transfer due to mass transfer between phases.

$$\Gamma_G \Delta h_{LG} + \Gamma_L \Delta h_{LG} = 0 \quad (2.14)$$

Another alternative for the energy balance is to put in on function of the internal energy. In this case, the balance both phases would be:

$$A_G \frac{\partial}{\partial t} \rho_G e_G + \frac{\partial}{\partial z} \dot{M}_G e_G = -p \frac{\partial}{\partial z} \frac{\dot{M}_G}{\rho_G} + P_G \dot{q}_w + \Gamma_G \Delta h_{LG} + \dot{M}_G g \sin \varphi \quad (2.15)$$

$$A_L \frac{\partial}{\partial t} \rho_L e_L + \frac{\partial}{\partial z} \dot{M}_L e_L = -p \frac{\partial}{\partial z} \frac{\dot{M}_L}{\rho_L} + P_L \dot{q}_w - \Gamma_L \Delta h_{LG} + \dot{M}_L g \sin \varphi \quad (2.16)$$

This balance seems easier to be solved in what respects to the complexity of the terms, but it has an important problem and that is that it could not be reduced to only one expression for the mixture. Consequently in case of using this method, two different balances must be solved at the same time, giving more complexity for solving in general disregarding the previous improvements.

In each balance of the mixture appear different types of densities, coming from mathematical simplification of the properties of both phases. The mixture density, impulse density and energy density are shown in the next three equations:

$$\rho_M = \varepsilon \rho_G + (1 - \varepsilon) \rho_L \quad (2.17)$$

$$\frac{1}{\rho_I} = \frac{x^2}{\varepsilon \rho_G} + \frac{(1 - x)^2}{(1 - \varepsilon) \rho_L} \quad (2.18)$$

$$\frac{1}{\rho_E^2} = \frac{x^3}{\varepsilon^2 \rho_G^2} + \frac{(1-x)^3}{(1-\varepsilon)^2 \rho_L^2} \quad (2.19)$$

This three balances gives a big picture of the problem, and helps to understand the importance and the role of the different principles that step in the study of the transient condenser. First is very important to have a really good estimation of the void for the two phase fluid. And then the problem diverge in two different branches, the pressure loss and the heat transfer, being the last one the more complicated to estimate and the more important.

2.4 Void fraction

“Void fraction is the foremost parameter in determining two-phase flow pattern transitions, two-phase heat transfer coefficients and two-phase pressure drops. Therefore, it is important to have a method that is both accurate and reliable over the whole range of mass velocities, flow regimes and reduced pressures” [5]. At the beginning of this study, I did not grasp the importance of having a good empirical approximation of the void, but when I started running some test with a preliminary program, I realized the sensibility of all the values estimated to the void.

At first I started working with a proposed heat transfer method in previous investigations. This method presented in the *Chapter of condensation J1 of the VDI Heat Atlas* [27] has its own empirical definition of void. But as the investigation advanced, I comprehended that this method was intended only for filmwise condensation, and in this case of study a complete condensation, probably giving different flow patterns, is pretended and observed. Also I tried to check references of the empirical definition of the void, and to see if it was tested for the working fluid propane, but I did not have any confirmation. Finally, the method was dismissed, so the first step after that was to find an empirical correlation of the void that suits the range of properties of this study.

The method to calculate the void fraction, must be suitable for condensation for horizontal tubes, must have been tested for propane and must be recommended for the mass flux and pressure range that MoNiKa condenser works. J. El Hajal, J.R. Thome and A. Cavallini published a method in 2003 [5] which fulfills all this requirements and also has the important feature that works for the whole range of flow regimes, since there is no way to confirm which flow pattern take place along the length of the tubes. This method is referred as the logarithmic mean void fraction, because it combines a homogenous void fraction ε_h and a non-homogeneous void fraction ε_{ra} with a logarithmic mean function.

$$\varepsilon_h = \left[1 + \left(\frac{1-x}{x} \right) \left(\frac{\rho_G}{\rho_L} \right) \right]^{-1} \quad (2.20)$$

$$\varepsilon_{ra} = \frac{x}{\rho_G} \left([1 + 0.12 (1 - x) \left[\frac{x}{\rho_G} + \frac{1 - x}{\rho_L} \right] + \frac{1.18(1 - x) [g \sigma (\rho_L - \rho_G)]^{0.25}}{G \rho_L^{0.5}}]^{-1} \right) \quad (2.21)$$

Equation (2.20) displays the homogenous void fraction. For the non-homogeneous void, the method chose the drift flux model of Rouhani and Axelsson [30] presented in equation (2.21). σ represents the surface tension, and G the total mass flux of liquid and vapor.

To obtain a correlation where the effect of pressure is correctly accounted, an interpolation between the two void fractions presented is needed, since both present accurate values for different pressure range. The equation (2.22) displays the logarithmic mean void fraction:

$$\varepsilon = \frac{\varepsilon_h - \varepsilon_{ra}}{\ln \left(\frac{\varepsilon_h}{\varepsilon_{ra}} \right)} \quad (2.22)$$

2.5 Pressure Loss

The pressure loss is commonly defined by the *Darcy–Weisbach equation* described in equation (2.23). K represents the total pressure loss coefficient, and is the sum of the friction losses, also called major losses, and the local losses. The first ones are the pressure losses that take place in the length of the pipes, the second ones occurs in components as valves, elbows, bends, etc. In this study the local losses were estimated and neglected later for being insignificant compared to the major ones. The subscript j stand for L (liquid) or G (gas), depending the state of the fluid referenced.

$$\Delta p_j = \frac{1}{2} \frac{K_j \dot{M}_j^2}{\rho_j A_j^2} \quad (2.23)$$

For the estimation of the pressure loss coefficient several correlations exist but, I tried to use some that are simple and reliable. I started with a ground settle by previous investigations on MoNiKa, and also by a MATLAB code programmed by Prof. Dr. Thomas Schulenberg named OTEST [19]. By testing and analyzing the ranges of application of the different empirical correlation, I finally choose to use the ones presented next.

Is important to know that the correlations changes in what respects from a fluid in single phase and one with two phases. The regime of the fluid, and some times of each phase, is important. To estimate if a fluid is in laminar or turbulent regime, the dimensionless number of Reynolds is used (2.24), and is defined as the ratio between the inertial forces and the viscous forces.

$$Re_j = \frac{\dot{M}_j d_{Hj}}{A_j \mu_j} \quad (2.24)$$

This expression is in function of the mass flow as contrasting with the common expression in function of the velocity. That is because it fits better for my study were the mass flow is a measured variable. μ is the dynamic viscosity.

The pressure loss coefficient (2.25) depends of the friction factor f , or also called Darcy–Weisbach friction factor, of the hydraulic diameter d_H , of the length Δz and the form loss coefficient ξ .

$$K_j = \left(\frac{f_j \Delta z}{d_{Hj}} + \xi \right) \quad (2.25)$$

In the case of a single phase fluid, the expresion for the friction factor at laminar regime used is the one deduced by Hagen–Poiseuille:

$$f_j = \frac{64}{Re_j} \quad (2.26)$$

It is consider that the Reynolds number for a laminar flow inside of a tube is $Re < 2000$, and for turbulent flow must be $Re > 2000$. There is a critical zone between $2000 < Re < 4000$, depending on the bibliography, and the values around this area are not really trustworthy.

For turbulent regime, it is important to distinguish between a smooth tube and a rough one. Normally the smooth tube is a theoretical definition and the rough tube is the regular used.

$$f_j = \frac{1}{\left[1.8 \log(Re_j) - 1.5 \right]^2} \quad (2.27)$$

$$f_j = \frac{1}{\left[2 \log \left(3.71 \frac{1}{\eta} \right) \right]^2} \quad (2.28)$$

Equation (2.27) is a correlation from Konakov [11] used for smooth tubes and in a range of $2300 < Re < 10^7$. Equation (2.28) presented by Nikuradse [15] works for tubes with roughness η in turbulent regime, it has the particularity that does not depends on the Re Number. The relative roughness (2.29) is defined by the ratio between the absolute roughness and the inner diameter of the tube.

$$\eta = \frac{\kappa}{d} \quad (2.29)$$

For the two phase fluid, I adopted the method by Lutz Friedel [6, 7]. This method uses the estimation of a single phase liquid and multiplies it by a correction factor which takes into account the distribution of gas and liquid phase.

$$\Delta p = \Phi_{Lo}^2 \Delta p_L \quad (2.30)$$

$$\Delta p = \Phi_{Lo}^2 \frac{1}{2} \frac{K_L \dot{M}^2}{\rho A^2} \quad (2.31)$$

The empirical factor for two phase Φ_{Lo}^2 definition is:

$$\Phi_{Lo}^2 = D + 3.43 x^{0.685} (1-x)^{0.24} \left(\frac{\rho_L}{\rho_G}\right)^{0.8} \left(\frac{\mu_G}{\mu_L}\right)^{0.22} \left(1 - \frac{\mu_G}{\mu_L}\right)^{0.89} Fr_L^{-0.047} We^{-0.0334} \quad (2.32)$$

Is a function of the quality x , the density and viscosity of both phases and the factor D :

$$D = (1-x)^2 + x^2 \left(\frac{\rho_L f_G}{\rho_G f_L}\right) \quad (2.33)$$

D depends on the friction factor of both phases, and they are defined by Friedel method as equation (2.34) for $Re < 1055$, and as equation (2.35) for $Re > 1055$.

$$f_j = \frac{64}{Re_i} \quad (2.34)$$

$$f_j = \left(0.86859 \ln \frac{Re_j}{1.964 \ln Re_j - 3.8215} \right)^{-2} \quad (2.35)$$

The two phase factor also is a function of the Weber and Froude dimensionless numbers. The first one (2.36) is defined as the ratio between the inertial forces and the surface tension of the fluid, the second one (2.37) as the ratio of the inertial forces and gravitational forces that takes action on the fluid.

$$We = \frac{d \dot{M}^2}{A_c^2 \rho_L \sigma_L} \quad (2.36)$$

$$Fr_L = \frac{\dot{M}_L^2}{A_c^2 g d \rho_L^2} \quad (2.37)$$

A_c is the cross section area, σ_L is the surface tension of the liquid and g is the gravitational constant acceleration.

2.6 Heat Transfer

In the energy balance, the heat transferred by the primary fluid to the secondary is needed to be predicted. For this purpose the Fourier law or law of heat conduction is presented as:

$$\dot{Q} = k A \Delta T_m \quad (2.38)$$

Where \dot{Q} is the heat rate transferred between both fluids trough the wall of the condenser, k is the overall heat transfer coefficient or thermal conductivity, A is the heat Exchange area between both fluids and ΔT_m is the arithmetic mean temperature difference defined:

$$\Delta T_m = \left(\frac{T_{o,a} + T_{i,a}}{2} \right) - T_p \quad (2.39)$$

Here T_p is the propane temperature, and is consider constant in the length of each Δz of discretization. $T_{o,a}$ and $T_{i,a}$ are the temperature of the air at the outlet and the inlet of the condenser respectively.

The product kA is defined as:

$$\frac{1}{k A} = \frac{1}{\alpha_i A_i} + \frac{(d_o - d_i)}{2 \lambda_w A_i} + \frac{1}{\alpha_o \eta_o A_o} + Rf \quad (2.40)$$

The first term in equation (2.40) refers to the heat convection inside the tube, in this case the convection in the propane, α_i is the inner heat transfer coefficient and A_i is the inner area of the tube. The second one is the conduction inside the walls of the tube, it depends on the geometry and the properties of the material, d_o and d_i are the outer and inner diameter respectively and λ_w is the thermal conductivity of the wall. The third term represents the convection outside the tube, in the air side, α_o is the outer heat transfer coefficient, A_o is the outer area of the tube and η_o is the surface efficiency.

R_f is the fouling resistance, in most industrial processes, heat exchanging fluids contain certain amounts of dissolved or suspended material or provide conditions favorable for the growth of biological organisms. Since the thermal conductivity of such deposits is low, their resistance to heat transfer may well exceed that of the clean fluids, resulting in significantly reduced heat exchanger performance [27]. In my study, I neglected the fouling resistance because the condenser is relative new and with almost no use, also there is no measure to try to estimate this value, and finally there are no reliable data for typically condensers that works with propane and this geometry.

For all heat transfer coefficients, the definition of the dimensionless Nusselt number is used:

$$Nu = \frac{\alpha d_h}{\lambda} \quad (2.41)$$

It is defined as the ratio between the convective heat transfer of a fluid and the conductive heat transfer. d_h is the hydraulic diameter and λ is the thermal conductivity of the fluid an inherent property of each fluid.

To calculate the Nusselt number, there are empirical correlations determined by experiments for numerous applications. The correlations have in common that they describe the Nusselt number as a function of the dimensionless numbers Re and Pr , Reynolds and Prandtl number respectively.

$$Re = \frac{w d_h}{\nu} \quad (2.42)$$

$$Pr = \frac{\mu c_p}{\lambda} \quad (2.43)$$

The Reynolds number was defined previously but here is in function of the velocity of the fluid w and his kinematic viscosity ν . The Prandtl number is the ratio between the momentum diffusivity and the thermal diffusivity of the fluid. c_p is the specific heat of the fluid.

2.6.1 Outer heat transfer coefficient – Air side

Is important to work with a correlation intended for a similar geometry and distribution as the condenser already installed. Likewise is important that the fluid was tested for that purpose, in this case air. The form and arrangement of the fins and tubes also need to be in the range of the experiments conducted in the investigation of the correlation. The Reynolds is important to be in range also.

As it was mentioned, the study starts with a method proposed by previous studies and developed in the VDI Heat Atlas, but the method for the heat transfer on the air side does not contemplate the type of fins used in MoNiKa, so I made a search for another method. The condenser is a plain fin condenser with horizontal round tubes, which is refrigerated by air. It has 4 row and 69 tubes per row. With this information the method by N. Kayansayan [14] was selected between another possibilities.

$$\alpha_o = \frac{Nu_{air} \lambda_{air}}{d_o} \quad (2.44)$$

The thermal conductivity of the air λ_{air} is a property known estimated with REFPROP, d_o is a constant of the tube and Nu_{air} is the only incognita.

This method presents that by the Colburn analogy [4]:

$$Nu = f(Re, Pr, flow\ geometry) \quad (2.45)$$

Consequently Kayasayan suggest this equation for the range of $0.5 < Pr < 100$:

$$Nu = C Re^m Pr^{1/3} \epsilon^n \quad (2.46)$$

The definition of the Colburn j factor for this case is:

$$j = \frac{Nu_{air}}{Re_{air} Pr_{air}^{1/3}} \quad (2.47)$$

Hence, from both previous equations:

$$j = C Re_{air}^{m-1} \epsilon^n \quad (2.48)$$

Where the flow geometry effect is represented by the exchange finning factor as recommended by McQuiston [13]:

$$\epsilon = \frac{A_o}{A_{bo}} \quad (2.49)$$

A_o is the total outside area per unit length and A_{bo} is the bare tube outside area per unit length, and both are defined like:

$$A_{bo} = \pi d_o (1 - t_{fin} z_{finm}) N n \quad (2.50)$$

$$A_{fin} = \frac{\pi d_o^2}{2} \left(\frac{4}{\pi} \frac{u_l}{d_o} \frac{u_t}{d_o} - 1 \right) z_{finm} N n \quad (2.51)$$

$$A_o = A_{bo} + A_{fin} \quad (2.52)$$

A_{fin} is the total area of the fins per unit length, z_{finm} is the density of fins per meter, t_{fin} the thickness of the fin, N the number of rows and n the number of tubes per row.

The geometrical properties of the bundle of tubes u_l and u_t is represented in figure Figure 2.7. The subscript l stands for the longitudinal direction parallel to the air flow, on the other hand, t stands for the transversal direction to the air flow.

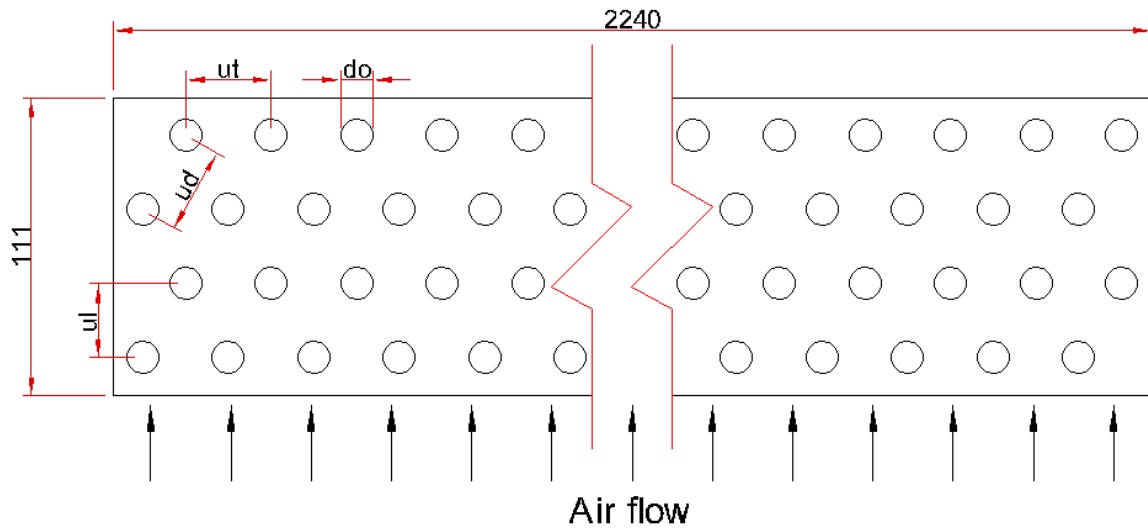


Figure 2.7 geometry and arrangement of the tube bundle in a fin

The Reynold number is recommended by the method to be calculated as:

$$Re_{air} = \frac{\dot{M}_{air} d_o}{A_{min} \mu_{air}} \quad (2.53)$$

Where A_{min} is the minimum flow area per unit length:

$$A_{min} = n (u_t - d_o) (1 - t_{fin} z_{finm}) \quad (2.54)$$

The method presents the values of the constant C and the exponentials $m-1$ and n in equation (2.48) that fits better to the data gathered in that study, but also mentions other methods like the study by McQuiston [13] and by Gray and Webb [9], and states that the exponent $m-1$ should be a value between -0.4 and -0.2. The following correlation was presented by Kayansayan:

$$j = 0.15 Re_{air}^{-0.28} \epsilon^{-0.362} \quad (2.55)$$

In the program, I used an exponent $m-1$ of -0.328 as it is used by Gray and Webb, and suggested by Kayansayan as a possibility in his investigation.

For the experiments the geometrical parameters varied in the ranges $2.39 < u_t/d_o < 3.15$, $2.07 < u/d_o < 2.67$, and $0.131 < (t_{fin}+u_{fin})/d_o < 0.425$, being u_{fin} the distance between fins. Also the range for the Reynolds number was $500 < Re < 30000$.

2.6.2 Surface efficiency

The surface efficiency is defined as the actual heat transfer for the fin and base divided by the heat transfer for the fin and base when the fin is at the same base temperature.

For the calculus of the surface efficiency, the method by Schmidt [23] presented by Wang and Chi [3] is used. The definition is the same for different authors:

$$\eta_o = \left(1 - \frac{A_{fin}}{A_o} (1 - \eta_{fin}) \right) \quad (2.56)$$

Where η_{fin} is the efficiency of the fins and is defined as:

$$\eta_{fin} = \frac{\tanh(m_{fin} \frac{d_o}{2} \phi_{fin})}{m_{fin} \frac{d_o}{2} \phi_{fin}} \quad (2.57)$$

Where:

$$m_{fin} = \sqrt{\frac{2 \alpha_o}{\lambda_{fin} t_{fin}}} \quad (2.58)$$

$$\phi_{fin} = \left(\frac{R_{eq}}{r} - 1 \right) \left[1 + 0.35 \ln \left(\frac{R_{eq}}{r} \right) \right] \quad (2.59)$$

$$\frac{R_{eq}}{r} = 1.27 \frac{u_t}{d_o} \left(\frac{u_d}{u_t} - 0.3 \right)^{\frac{1}{2}} \quad (2.60)$$

Where u_d is the distance between tubes from different rows represented in Figure 2.7. λ_{fin} is the thermal conductivity of the material that the fin is made off, in this case Al-Hydro.

2.6.3 Inner heat transfer coefficient – Propane side

For the prediction of the inner heat transfer coefficient, there are two different sets of correlations, one for single phase fluid and another one for two phase. Both predict the Nusselt number which is

used to calculate the heat transfer coefficient. For this purpose, the Nusselt definition on equation (2.41) is used.

In the case of single phase fluids and $Re < 2000$ (laminar flow), the correlation presented in the book Fundamentals of Heat and Mass Transfer [10] is used, which considers a constant temperature in the wall of the tube:

$$Nu = 3,6568 \quad (2.61)$$

For turbulent flow in the range of $2000 < Re < 10000$, called as a range where the turbulent regime is not full developed, the correlation by Gnielinski [8] is used:

$$Nu = \frac{(f/8) (Re - 1000) Pr}{1 + 12,7 \sqrt{f/8} (Pr^{2/3} - 1)} \quad (2.62)$$

For the friction factor f , two correlations are used, the first one by Konakov [11] for smooth pipes presented in equation (2.27) and the second one presented by Nikuradse [15] in Equation (2.28).

In the range of a fully developed turbulent regime with $Re > 10000$, the correlation given by Dittus-Boelter is used. The first one for smooth pipes and the second one for pipes with a relative roughness η :

$$Nu = 0,023 Re^{0.8} Pr^{1/3} \quad (2.63)$$

$$Nu = 0,023 Re^{0.8} Pr^{1/3} \left(1.87 + 0.54 \log \left(1000 \frac{r}{d_H} \right) \right) \quad (2.64)$$

For two phase fluids, many correlations were tested. The first one was the one proposed by previous investigations and presented in the chapter J1 of the Heat Atlas [27], but then dismissed because it was pretended for film condensation only.

The method used in the program is the one developed and improved by Shah [21, 22], other methods tested where the one proposed by Akers et al. [2] and by Collier in [1].

Shah presented in 1979 a method where a heat transfer coefficient for liquid single phase is multiplied by an empirical two phase factor to obtain the final coefficient for two phases. This empirical factor is a function of the pressure, the critical pressure and the quality of the fluid. In 2009 the method was improved, and the previous correlation was modified by a viscosity ratio factor and set as a formula only for the turbulent regime. The rest of the improvement of the method was on the development of other two formulas for the mixed and laminar regime, achieving better results in a wider range of application.

The correlation uses these two equations:

$$\alpha_I = \alpha_L \left(1 + \frac{3.8}{Z^{0.95}} \right) \left(\frac{\mu_L}{14\mu_G} \right)^{(0.0058+0.557 p_r)} \quad (2.65)$$

$$\alpha_{Nu} = 1.32 Re_L^{-1/3} \left[\frac{\rho_L(\rho_L - \rho_G)g \lambda_L^3}{\mu_L^2} \right]^{1/3} \quad (2.66)$$

For the liquid heat transfer coefficient α_L , a variation of the Dittus-Boelter equation is presented by the method:

$$\alpha_L = 0,023 Re_L^{0.8} Pr_L^{0.4} \frac{\lambda_L}{d_H} \quad (2.67)$$

The correlating parameter Z is defined as:

$$Z = \left(\frac{1}{x} - 1 \right)^{0.8} p_r^{0.4} \quad (2.68)$$

p_r is the reduced pressure:

$$p_r = \frac{p}{p_{crit}} \quad (2.69)$$

The different regimes are determined by the value of J_G , the dimensionless vapor velocity defined as:

$$J_G = \frac{x G}{(g di \rho_G (\rho_L - \rho_G))^{0.5}} \quad (2.70)$$

In regime I, called turbulent, the heat transfer coefficient is displayed in equation. For Regime II and III, mixed and laminar respectively, equations (2.72) and (2.73) define it.

$$\alpha_i = \alpha_I \quad (2.71)$$

$$\alpha_i = \alpha_I + \alpha_{Nu} \quad (2.72)$$

$$\alpha_i = \alpha_{Nu} \quad (2.73)$$

Regime I occurs when:

$$J_G \geq 0.98 (Z + 0.263)^{-0.62} \quad (2.74)$$

The boundary between regime II and regime III is determined as follows. Regime III occurs when:

$$J_G \leq 0.95 (1.254 + 2.72 Z^{1.249})^{-1} \quad (2.75)$$

These regimes are defined for different pattern flows, such as mist, Annular, Intermittent, Stratified-Wavy and Stratified. Moreover, the study was verified for 24 fluids including propane.

3 Programming and simulation

3.1 REFPROP

“REFPROP is a program developed by NIST, calculates the thermodynamic and transport properties of industrially important fluids and their mixtures. These properties can be displayed in Tables and Plots through the graphical user interface. It implements three models for the thermodynamic properties of pure fluids: equations of state explicit in Helmholtz energy, the modified Benedict-Webb-Rubin equation of state, and an extended corresponding states (ECS) model” [17].

REFPROP has the purpose of providing accurate values of the physical properties of the fluids that are used in the simulation in each time lapse. So it is important not only to be accurate but also that could have a dynamic interaction with the program.

3.2 Simulink

“Simulink [25] is a block diagram environment for multidomain simulation and Model-Based Design. It supports system-level design, simulation, automatic code generation, and continuous test and verification of embedded systems. Simulink provides a graphical editor, customizable block libraries, and solvers for modeling and simulating dynamic systems. It is integrated with MATLAB [24], enabling you to incorporate MATLAB algorithms into models and export simulation results to MATLAB for further analysis” [26].

It was a requirement for the thesis to use the Simulink platform for the development of the transient prediction program. Without previous experience with the program, the first steps were to get used to the program the faster possible, and to learn how to model ODEs with a focus in fluid and thermodynamics. For this purpose videos and tutorials from Simulink help documentation and webpage where used.

The first attempt was to use the Two Phase block library that the Simulink has since a couple of versions, but it is not much flexible, correlations cannot be changed and with low knowledge about the program it was difficult to use. So instead I choose to use the program with the common logical blocks and taking advantage that Simulink was designed to have excellent communication with MATLAB, many blocks where programed in MATLAB.

Simulink has the possibility of choice between different types of solvers for the ODEs, and is possible to adjust discretization on time by choosing between a fixed time step or a variable time step. The last one is an automatic feature of the program that works really well, but of course it is not failsafe in all the cases.

3.3 Code beginning

The objective of the program is to solve the governing balance presented in chapter 2 given the inputs for each time, and as a result predict the transient behavior of the fluid on the outlet.

As it was mentioned in chapter 2, the effect of the difference in height between tubes inside the condenser was estimated and defined as negligible compared to the others effects. With this in mind, is important to assume that the distribution of mass flow inside of the 69 tubes is equal. Consequently,

if the mass flow between the 4 heat exchange areas is equally distributed because of the symmetry of the geometry of the condenser, and the mass flow is also equally distributed in each tube, the model is reduced to a tube with a length L . The properties of the fluid are constant in the cross section in each space differential.

The problem can be resumed as a control volume of a single tube with one dimension, with three variables, mass flow \dot{M} , pressure p and enthalpy h . All variables defined as inputs, and unknown in the output of the condenser, therefor will be simulated as an explicit model. To solve I have 3 different balances and the 3 equations of the densities in the case of two phase flow.

The control volume is discretized in cells and nodes. In the nodes, the pressure, enthalpy, temperature and density are defined. In the cells, mass flow, pressure losses, heat flux and geometry properties as perimeter, cross section and height are defined. The discretization starts with the entrance node in which pressure, enthalpy and mass flow is defined, and continues with the first cell.

Since Simulink works with blocks, my idea is to divide the tube in cells, and each cell will be represented by a block called subsystem, which will be constitute by others blocks and subsystems, making that way the model hierarchy. First, there is the general model, were all input variables, geometric properties and constant properties of the fluids are input. All this inputs are distributed to the outer heat transfer Block and to all the Cells Subsystems.

The Figure 3.1 is useful to have a better understanding of the hierarchy of the model while talking about the structure of the program inside Simulink:

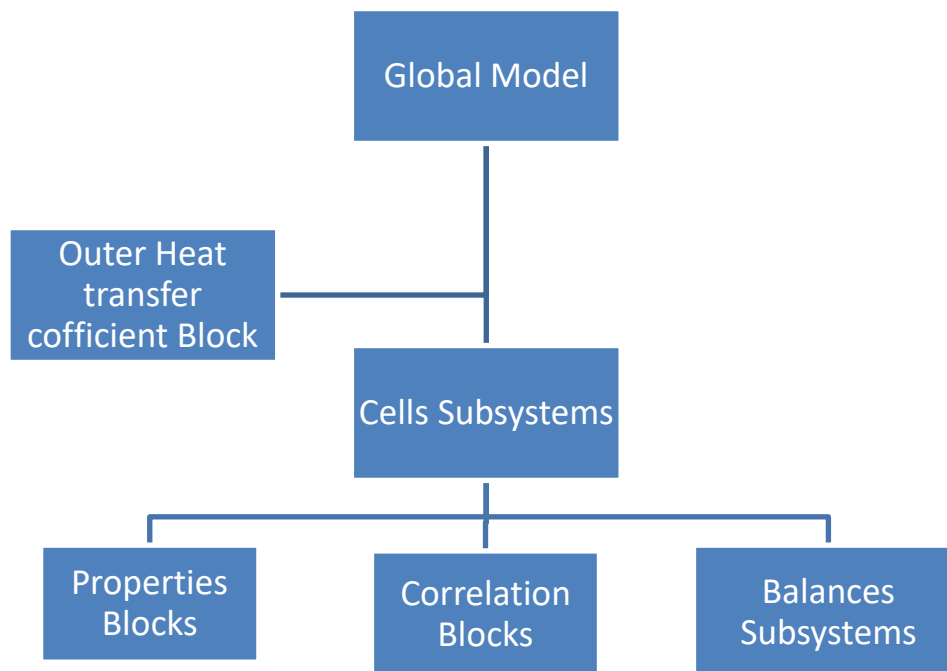


Figure 3.1 model hierarchy

The outer heat transfer coefficient is independent from the block cells since the heat transfer coefficient depends on the geometric properties of the condenser and on the properties of the air. The first ones are constant in all the length of the tube by symmetry. The second ones are properties that depend on the pressure and temperature of the air. In the case of viscosity, thermal conductivity and

number of Prandtl, a sensibly study between the possible range of air pressure was held, and the variation was negligible, so the ambient pressure is used with a mean value between inlet (ambient temperature) and outlet temperature, to call these properties from REFPROP. The outlet temperature is measured by one sensor per fan, therefore a mean value between this three readings is used.

For the retrieving of physical properties from REFPROP, the *refprop.m* function provided by NIST is used in MATLAB to preload the properties needed in the workspace. Two independent properties of the fluid are used to calculate the value needed by the equations of state on REFPROP. For invoking the function, the following procedure is executed:

$$result = refpropm(prop_req, spec1, value1, spec2, value2, substance1)$$

Here the first input are the properties required to be calculated, spec1 and spec2 are the independent properties of the fluid to be used, value1 and value2 are the numerical values of this properties and substance1 is the fluid to work with. It is important to watch carefully in which properties the different inputs have to be provided, because it does not use the MKS system for all properties. In the case of the fluid, the input can be a pure substance, a mixture already defined in REFPROP (like air), or an original mixture of substance.

The density of the air at the entrance is needed to calculate the mass flow at the inlet, for this a mean value of ambient temperature and pressure in the whole time range of the test are used. The sensibility of the density to the variation of the temperature in the test days is very small: to grasp an idea, in a variation from 0°C to 10°C the density value differs by 3.5%. The variation in ambient temperature in the cases tested were less than 1°C.

Next in hierarchy are the Cell Subsystems. Each one of these represents a different cell in the model, therefore they are responsible of the discretization in space. There are three different types: the initial cell, the middle cells, and the final cell. The difference between subsystems are small, like different form loss to the initial cell, different number of outputs to the final cell, and there is no possibility to calculate the variation of density in the initial cell since there is no input information about the previous node.

Inside the Cell Subsystems are different types of blocks such as properties blocks which calculate, by definition or provided from REFPROP, physical properties of the fluid according to the input values of each cell. Also there are correlation blocks, which basically solve the empirical correlations explained in section 2. And finally I made different Balance Subsystems that solve logically the different balance using the outputs of the previous two types of blocks, plus the Cell Subsystem inputs.

3.4 Two Phase fluid tables

At the beginning of the development of the program, I start with the knowledge that REFPROP and MATLAB could communicate really well. So knowing also that MATLAB and Simulink work together, I explore the possibility to connect Simulink and REFPROP in real time. In Simulink exists a type of block which includes MATLAB code in models that generate embeddable C code, called

MATLAB function. The problem was that the functions used to work with REFPROP are incompatible with the block.

After researching for new options to acquire the physical properties for my program, I found a function on MATLAB called “twoPhaseFluidTables”. This function obtains fluid properties from REFPROP or CoolProp, and order them in tables, which are a function of pressure and normalized internal energy \bar{e} . The code for the function is:

*propaneTablesMonika = twoPhaseFluidTables (uRange, pRange, mLiquid,
mVapor, n, substance, installPath)*

Here the uRange is the internal energy range of values, pRange is the pressure range of values, mLiquid and mVapor are the number of rows or divisions for the internal energy range, n is the number of columns or divisions for the pressure range, substance is the fluid required and installPath is the path of the REFPROP or CoolProp in your computer.

The tables are organized in two sections, one for subcooled liquid and the other one for superheated vapor. Each section contains the following properties of the fluid:

Specific volume, v [m ³ /kg]	Thermal conductivity, k [W/(m*K)]
Specific entropy, s [kJ/(kg*K)]	Prandtl number, Pr [-]
Temperature, T [K]	Saturated liquid or vapor specific internal energy, e_{sat} [kJ/kg]
Kinematic viscosity, ν [mm ² /s]	Specific internal energy e [kJ/kg]

Table 3.1 Two phase fluid tables properties

The normalized internal energy is defined as:

$$\bar{e} = \frac{e - e_{min}}{e_{L sat} - e_{min}} - 1 \quad \begin{matrix} e_{min} \leq e \leq e_{L sat} \\ (Subcooled liquid) \end{matrix} \quad (3.1)$$

$$\bar{e} = \frac{e - e_{L sat}}{e_{G sat} - e_{L sat}} = x \quad \begin{matrix} e_{L sat} \leq e \leq e_{G sat} \\ (Two phase mixture) \end{matrix} \quad (3.2)$$

$$\bar{e} = \frac{e - e_{max}}{e_{max} - e_{G sat}} + 2 \quad \begin{matrix} e_{G sat} \leq e \leq e_{max} \\ (Superheated vapor) \end{matrix} \quad (3.3)$$

The system of the function in which the tables are organized in function of p and \bar{e} is really interesting and its main purpose is to gain a good organization. As it is displayed in Figure 3.2, the grid arrangement on the right is better for table organization, where L and V are abbreviations for liquid and vapor.

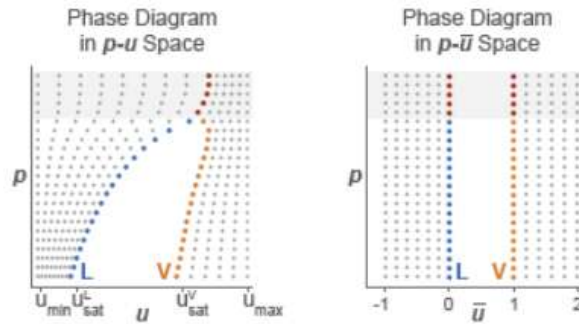


Figure 3.2 difference in phase diagrams using internal energy and normalized internal energy [26]

It is important to recall that Simulink and MATLAB Workspace can share data. This means that every variable loaded in the workspace of MATLAB, before running the program in Simulink, can be used or called by the functions in Simulink. Also that Simulink can write variables in the MATLAB Workspace. Consequently the two phase tables generated in MATLAB can be used by a block named “Lookup Table”. This block can search inside the tables with a given parameter of p and \bar{e} , it has the advantage of being a fast method and the possibility of choosing the extrapolation, interpolation and index search method. This last feature allows me to choose between different methods of interpolation and extrapolation, from slower and accurate to simpler and faster ones. The index search depends on the arrangement of the tables.

This solution for the problem of communication between programs becomes also a great improvement of the code, because the method for the generation of tables is really simple and, if they are well used, it has the same reliability as calling the properties from REFPROP. But the better upgrade is for the computing time, the use of lookup tables is much faster than calling the REFPROP each time you need a property.

3.5 Functional flow of the Program

The Simulink needs to solve all the blocks and subsystems to change and start solving the next time step. In case there is any error, the program stops in the actual time step, and presents the result until that time. It also states which the error is and sometimes a possible solution.

Figure 3.3 shows the flow diagram of the program. The first step is to preload into MATLAB the Two Phase Tables and the air properties. For that, I made a subroutine in MATLAB, so is necessary to run it first. In this subroutine, it is possible to change and check the p and \bar{e} range, the number of divisions per range and the fluid. Also is important to check that the pressure and temperature of the air is matching with the ones of the input data.

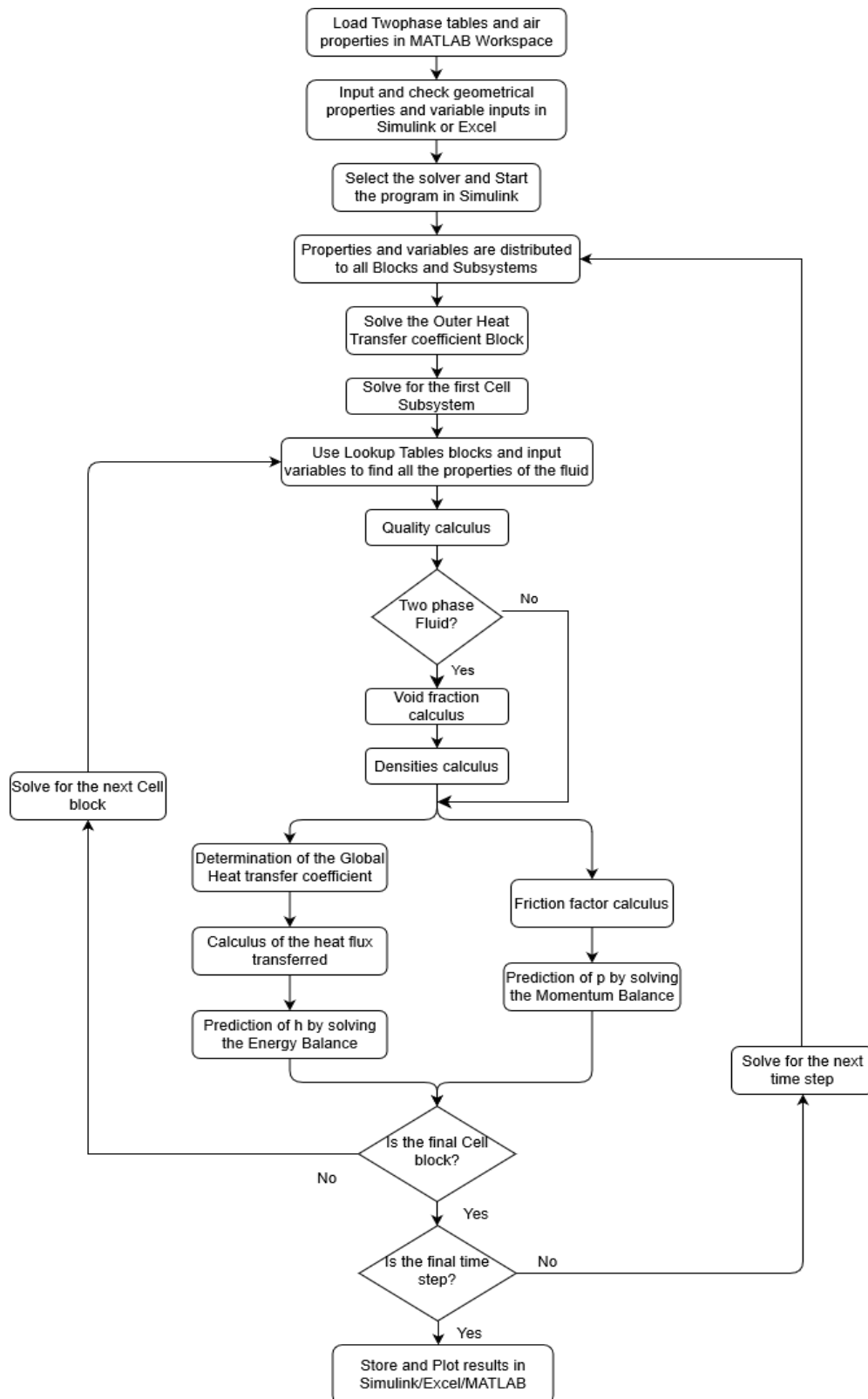


Figure 3.3 Flow diagram of the program

All the properties must be input on MKS system of units. For reference, each input and output field has the appropriate unit that must be used. The only exception is the pressure, which is given in

MPa by the sensor and needs to be input in that unit to search in the lookup table block. Consequently, it enters into the first Cell Subsystems in MPa, is used by the lookup table block and then converted to Pa for solving the rest of the tasks. Figure 3.4 displays how the Cell Subsystems are designed in the program, the inputs, outputs and how they are connected with next cell.

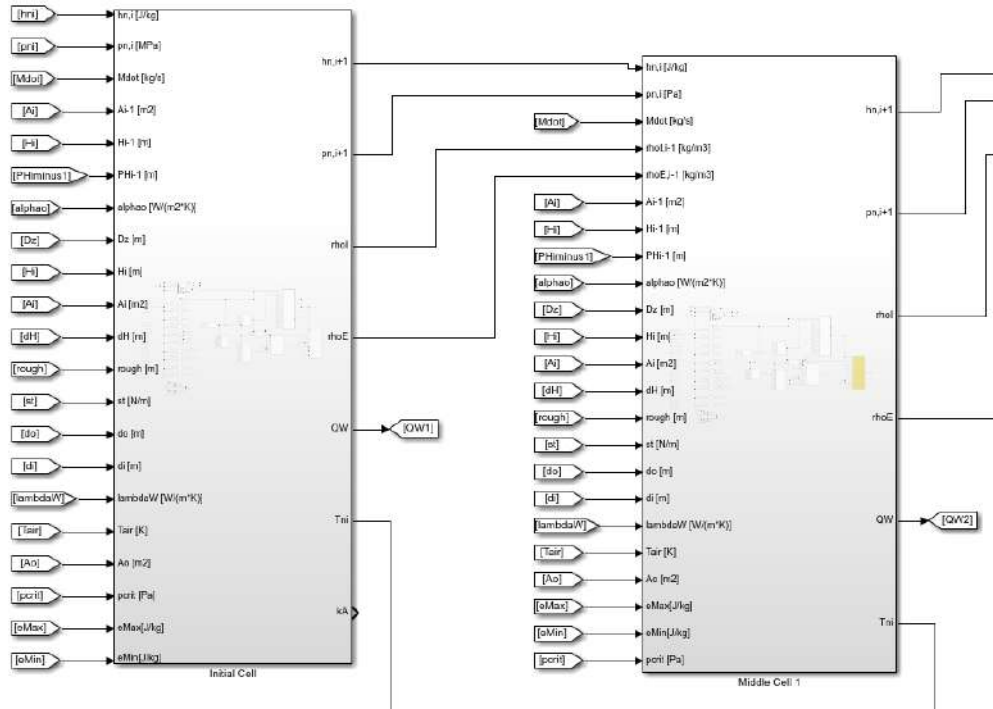


Figure 3.4 Cell Subsystem

Inside each Cell subsystem, the first action is to search for the properties of the fluid in the Two phase tables. From all the properties listed in Table 3.1, entropy is not used, and all the rest, with the exception of the temperature, are needed under saturation conditions. This means that the pressure is sufficient information to get almost all properties. After getting the properties, the quality, internal energy and normalized internal energy are calculated. With the last one, the temperature can be obtained. Note that if the fluid has two phases, the pressure is sufficient to obtain the temperature, but to know this it is necessary to first calculate the quality.

With the value of the quality, the state of the fluid is defined. In the case of a single phase fluid, all properties to solve the correlations and balances are known. For a two phase fluid, first is needed to calculate the void fraction and the different densities. For both aims, a MATLAB function block is used. These blocks have the correlations and formulas presented in section 2. The next step is solving the balances and correlations needed for that.

In section 2, I presented 3 different balances: mass, momentum and energy. The discretized form of the mass balance (2.6) bearing in mind that the time dependent term is neglected is:

$$\dot{M}_i^n - \dot{M}_{i-1}^n = 0 \quad (3.4)$$

Where the subscript i refer to the actual node or cell and the upper index n refers to the actual time step. Equation (3.4) shows that there is no need for solving the mass balance in the program, just known that the mass entering each cell is the same. Since there is no change in time or space in the mass flow, I am going to skip the subscripts and upper index to refer it. Also properties like the cross section area or the height, which do not change with time, do not have the upper index n .

In the case of the momentum balance, the discretized form of the equation (2.9) multiplied by $\frac{\Delta z}{A_i}$ is:

$$\frac{\Delta z}{A_i} \frac{\partial}{\partial t} \dot{M} + \dot{M}^2 \left(\frac{1}{A_{i+1} A_i \rho_{L,i+1}} - \frac{1}{A_i^2 \rho_{L,i}} \right) = -(p_{i+1}^n - p_i^n) - \frac{1}{2} \frac{K_i \dot{M}^2}{\rho_j A_i^2} - g \rho_{M,i+1} \Delta H \quad (3.5)$$

The time dependent term is neglected, and so the predicted pressure is defined as:

$$p_{i+1}^n = p_i^n - \frac{1}{2} \frac{K_i \dot{M}^2}{\rho_j A_i^2} - g \rho_M \Delta(H_{i+1} - H_i) - \dot{M}^2 \left(\frac{1}{A_{i+1} A_i \rho_{L,i+1}} - \frac{1}{A_i^2 \rho_{L,i}} \right) \quad (3.6)$$

Since there is no density defined in the first node, because only pressure, enthalpy and mass flow are defined at the entrance, the last term is neglected in the first cell block. The term of the gravity force is included in the program, but in the case of study of MoNiKa condenser is negligible, therefore there is no height input. The pressure loss coefficient K is calculated by a MATLAB block which has all the correlations presented in section 2.5. It is a simple code that depending the quality calculated previously using the correlations for single or two phase to determine K .

For the energy balance, the discretized form of the equation (2.13) multiplied by Δz is:

$$\begin{aligned} \rho_{M,i+1} V_i \frac{(h_{i+1}^n - h_{i+1}^{n-1})}{\Delta t} + \dot{M}(h_{i+1}^n - h_i^n) + \frac{\dot{M}^3}{2} \left(\frac{1}{A_{i+1}^2 \rho_{E,i+1}} - \frac{1}{A_i^2 \rho_{E,i}} \right) \\ = V_i \frac{(p_{i+1}^n - p_{i+1}^{n-1})}{\Delta t} + P_{H,i} \Delta z \dot{q}_{w,i} + A \rho_{M,i} \dot{Q}_s + \dot{M} g \Delta H \end{aligned} \quad (3.7)$$

The pressure time dependent term was already neglected in section 2 and also there is no heat source inside the fluid such that \dot{Q}_s is equal to zero. And so, the final expression to solve is:

$$\frac{(h_{i+1}^n - h_{i+1}^{n-1})}{\Delta t} = \frac{1}{\rho_{M,i+1} V_i} \left[\dot{Q}_i + \dot{M} g \Delta H - \dot{M} (h_{i+1}^n - h_i^n) - \frac{\dot{M}^3}{2} \left(\frac{1}{A_{i+1}^2 \rho_{E,i+1}} - \frac{1}{A_i^2 \rho_{E,i}} \right) \right] \quad (3.8)$$

The balance is presented in this form because is easier to get the idea of how it is solved by Simulink. To solve the time dependent term, an Integrator block from Simulink is used. This block integrates the input signal and saves its output to use in the next time step. It can use different numerical integration methods to compute the output, all of them have advantages in different applications.

In my case, I use a variable step solver, the ode45 (Dormand-Prince), which computes the model's state at the next time step using an explicit Runge-Kutta (4,5) formula (the Dormand-Prince pair) for numerical integration. It is a one-step solver, and therefore only needs the solution at the preceding time point [26].

I did not have the opportunity to do a deep comparison and analysis of the performance of different solver and type of step with my program. The time step is relatively small and the computational times are not really large. Nevertheless in the case of a bigger system, or larger set of inputs, maybe there is room to improve with another more adequate solver so that computational times do not get excessively high.

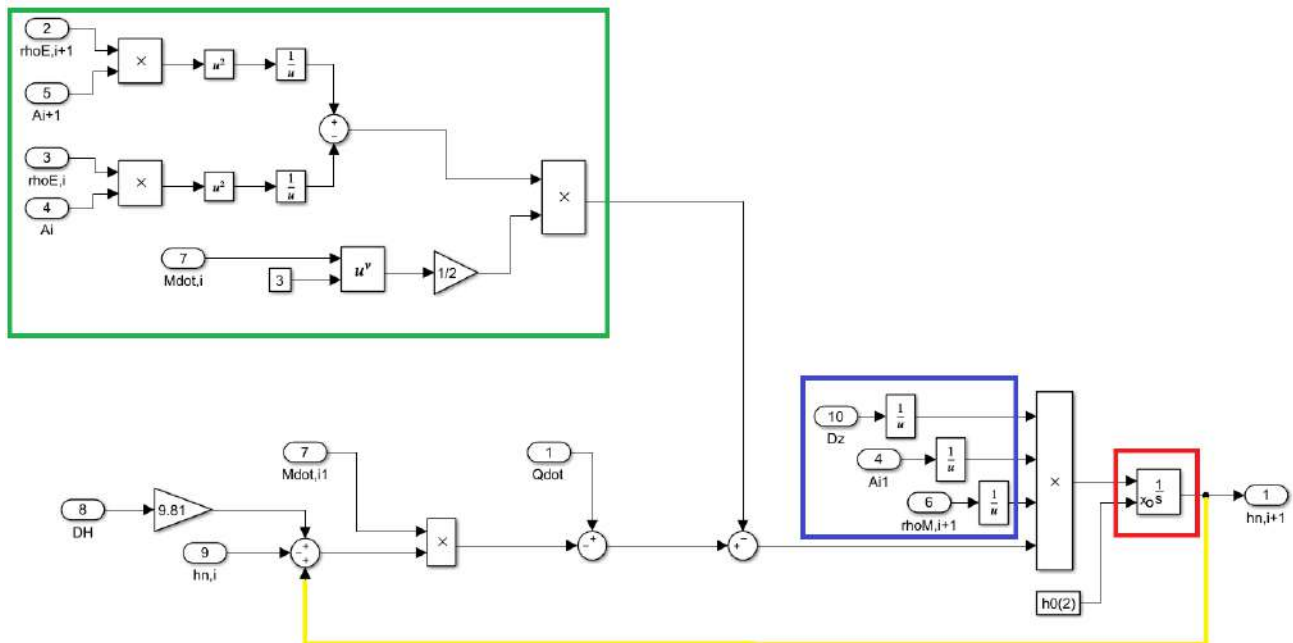


Figure 3.5 Energy balance subsystem diagram

Figure 3.5 shows the block diagram of the Energy balance subsystem. The red square holds inside the integrator block, and $h_0(2)$ is the initial condition for the integrator. In this case, I tried to

insert an external value added manually in MATLAB, because the accuracy of this value has a big impact on the time during which the integrator gets stable. I also tried to get h_i^n as initial value, which works better if you don't know the steady state for the first input value. The fluctuation on the output due to this effect is in the order of the 20 seconds.

The blue square indicates the variables multiplying the brackets in equation (3.8), the green square contains the last term inside the brackets, while DH is ΔH which is 0 for this case. The feedback loop is marked on orange. The blocks with an x inside are product blocks, multiplying all input variables.

3.6 First simulations

At the beginning, the model was formed by three cell subsystems, an initial one, the middle and the final one. It was meant this way to keep the model simple until all blocks and correlations works. It helped a lot to work this way because changes in the logic structure or boundary conditions in the blocks were implemented and tested way much faster than having a larger model. As more complex the model gets, the more boundaries it needs to handle.

The first time running the program I encounter several bugs in the code, it took me some days to debug all of them. The Simulink and MATLAB helped a lot with the task because for easy bugs like misspells or wrong use of functions, they mark the error and usually suggest a solution. After debugging the simple error, some missing boundaries were added, most of them referring to quality and void fraction ranges of MATLAB function blocks.

After that I encounter a problem more specific to MATLAB and Simulink. The thing is when using the MATLAB function block, the MATLAB Coder creates a C-code and then compiles/builds this code. For generating the C-code, the compiler needs to know which datatypes are used inside the function. As default, the coder assumes that the data is real and not complex. Complexity is a type in (Embedded) MATLAB, not an attribute. This is different from MATLAB, of course, where complexity changes at system run-time [26]. This description was found given by MathWorks support team in his forums.

I started having numerous errors when compiling the program, before the program starts to run in Simulink. Unfortunately, these types of errors were not displayed with location and possible solution. Taking in mind the issue described in the previous paragraph, I started a reduced MATLAB code with the objective of debugging the MATLAB code written for Simulink. I call this reduced version the Debugger version. Basically it is a MATLAB code that contains all the code previously written for the different blocks and all the properties and inputs necessary to run.

The first task of the debugger code was to check with real values the performance of the code and make an analysis of the results and try to narrow down where the errors were. At first I found a complex value that needed to be fixed in the code. But after that, all the values were real and inside a logical range. Knowing this, I rewrite the MATLAB function blocks and tried to run the program in Simulink again but the errors persist during the compiling task.

After running several tests and searching for an answer by forums of the program, I found out that the problem was not only with the functions giving complex values but also with the functions that

have a possibility of giving a complex value and is not specified. These functions in my code were mostly logarithms and pair fraction exponentials like square roots.

There were two solutions for this, the first one was to make the coder aware that each of these functions can present a complex value as an output, and the second was to ensure that each function input always be in the range where the function does not get complex values. The last proposal was implemented in the code, and so all logarithms have a minimum input of 1 and all pair fraction exponentials a minimum input of 0.

With this fix, the program could finish the compilation and the run. The first results were obtained and with that the first analysis to improve the model began.

4 Results and Validation

4.1 Data input

The geometrical properties of the condenser were retrieved of blueprints and documentation of the suppliers. These are properties as diameter of the tubes, quantity of tubes, inner roughness of the tubes, distance and arrangement of the tube bundle, size and thickness of the fins, etc.

For the properties of the fluid, all the data used for the test and validation was gathered in different test runs of MoNiKa, all of them with a throttling valve working instead of a turbine, as was stated in section 2.

The main idea was to realize tests, where the whole system could work in 3 stationary load points: 100% load, 70% load and 50% load. The test were in charge of all the Team working on MoNiKa at the ITES and all the data management was in charge of my colleague Luciano Gardella.

For the data gathering, temperature and pressure sensors are installed in the inlet and outlet of the condenser. Also there is a mass flow sensor for the entire primary fluid circuit. However, for the prediction with the program, enthalpy, pressure and mass flow are necessary.

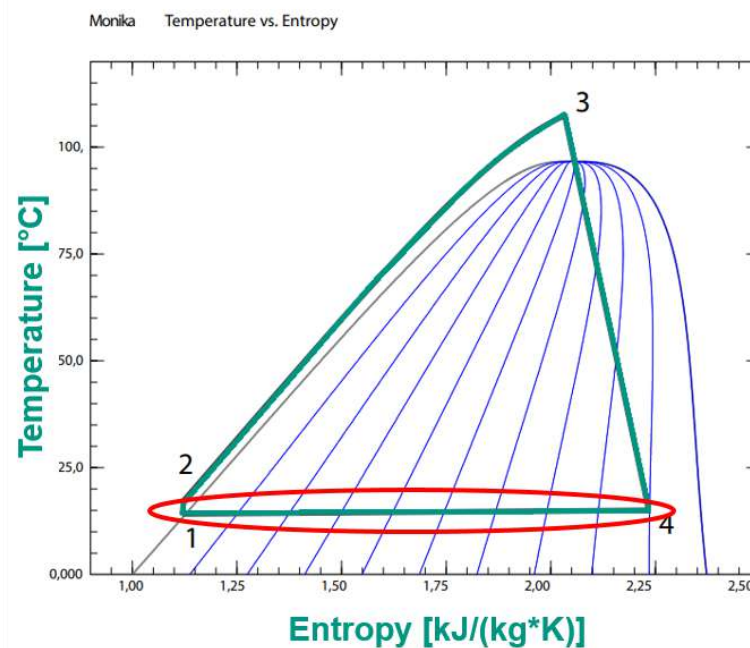


Figure 4.1 T-S diagram of MoNiKa, condensation zone of the cycle is marked in red

Since the data gathered in the test shows that the fluid in the point 1 is subcooled liquid, it is possible to obtain the enthalpy on that point with the pressure and temperature measured. However, is not the same for the point 4, because is inside the saturation zone and pressure and temperature are bounded, and so the quality of the fluid is necessary to obtain the enthalpy at the entrance of the condenser. There is no sensor to measure the quality or any other property than pressure and temperature in point 4, therefore the best option to obtain the input enthalpy for the study was to take the values of pressure and temperature of the point 3, and establish the enthalpy on that point. Then with the assumption that the throttling valve is isenthalpic and neglecting the heat losses from 3 to 4, I consider that the enthalpy on 3 is equals to the enthalpy on 4. The heat losses in the tubes from 3 to 4 were estimated for this assumption and neglected because of the insignificant impact on the

value. This should be taken in account as an input error or even as a model error, which is impossible to quantify with the present data.

For the retrieval of the air properties from REFPROP, an average temperature between ambient and the temperature measured at the outlet is used in MATLAB before starting the program. Inside the program, since the temperature of the air decreases in each tube row, I divided the total ΔT_{air} in 4 sections, so I can get a better approximation than using a single average temperature value for all the condenser. I used a linear division for this purpose knowing that probably the variation of air temperature in the condenser is different, but I only have two measures, and I couldn't find any bibliography about this issue. It is needed to be kept in mind the fact that the outlet air temperature in the data used is measured with only one sensor near the fan and that the air distribution inside of the condenser is unknown, these two facts induce an input error in a sensible value to the model.

The final test from which the data was taken for the final results in this study, was an almost 24 hours test. In this test the heat exchanger and the condenser are consider to reach a stationary flow for each load point proposed, but the pumps only reach a quasi-stationary flow.

The first objective was to run tests of the program with data from the stationary points and to do a verification and validation of the model first for this kind of regime. This was proposed because it is easier to run tests and analyze results with less entries, which is the case of a stationary regime where the input is the same for each variable all the time. Periods of time where the stationary points were reached were selected, and the mean values were obtained. All the values are presented with the relative error of each sensor installed in MoNiKa. The data used for this stationary tests is resumed in the following table:

100%				70%				50%			
Propane				Propane				Propane			
\dot{M}	2.866	kg/s		\dot{M}	2.032	kg/s		\dot{M}	1.451	kg/s	
\pm	0.003		0.10%	\pm	0.002		0.11%	\pm	0.002		0.11%
T_{in}	14.60	$^{\circ}\text{C}$		T_{in}	10.95	$^{\circ}\text{C}$		T_{in}	7.71	$^{\circ}\text{C}$	
\pm	0.18		0.06%	\pm	0.18		0.06%	\pm	0.18		0.06%
P_{in}	0.72	MPa		P_{in}	0.66	MPa		P_{in}	0.60	MPa	
\pm	0.01		1.38%	\pm	0.01		1.53%	\pm	0.01		1.68%
h_{in}	557	kJ/kg		h_{in}	556	kJ/kg		h_{in}	551	kJ/kg	
\pm	3		0.62%	\pm	3		0.61%	\pm	3		0.58%
T_{out}	13.82	$^{\circ}\text{C}$		T_{out}	10.40	$^{\circ}\text{C}$		T_{out}	7.25	$^{\circ}\text{C}$	
\pm	0.18		0.06%	\pm	0.18		0.06%	\pm	0.18		0.06%
P_{out}	0.722	MPa		P_{out}	0.658	MPa		P_{out}	0.602	MPa	
\pm	0.003		0.42%	\pm	0.003		0.46%	\pm	0.003		0.50%
h_{out}	235	kJ/kg		h_{out}	226	kJ/kg		h_{out}	218	kJ/kg	
\pm	0.5		0.20%	\pm	0.5		0.21%	\pm	0.5		0.21%
Air				Air				Air			
$T_{\text{air in}}$	0.98	$^{\circ}\text{C}$		$T_{\text{air in}}$	0.68	$^{\circ}\text{C}$		$T_{\text{air in}}$	-0.02	$^{\circ}\text{C}$	
\pm	0.15		0.06%	\pm	0.15		0.06%	\pm	0.15		0.05%
$T_{\text{air out}}$	6.8	$^{\circ}\text{C}$		$T_{\text{air out}}$	5.1	$^{\circ}\text{C}$		$T_{\text{air out}}$	3.4	$^{\circ}\text{C}$	
\pm	1.1		0.39%	\pm	1.1		0.40%	\pm	1.1		0.40%

Table 4.1 Stationary points and values for validation

For the transient validation, all the data that was taken in the final test was analyzed in search of range of values suitable for the validation of the program. In Figure 4.2 the values of the propane temperature during the test are shown. Between 20000 s and 30000 s the MoNiKa reaches the first quasi-stationary regime for the 100% load, then between 30000 s and 52000 s for the 70% part load, after that from 56000 s to 70000 s the 50% and finally there is the shutdown of the cycle. The idea is to validate for transients that represents load changes of the cycle. In Figure 4.2 and Figure 4.3 we see that there are four transients that fulfill that requirement. The first one is at the beginning of the test, when the cycle goes from 0 to 100%, this case is not used because it is a long transient that contains several effects which are not being represented in the model, like the variation of the fan speed.

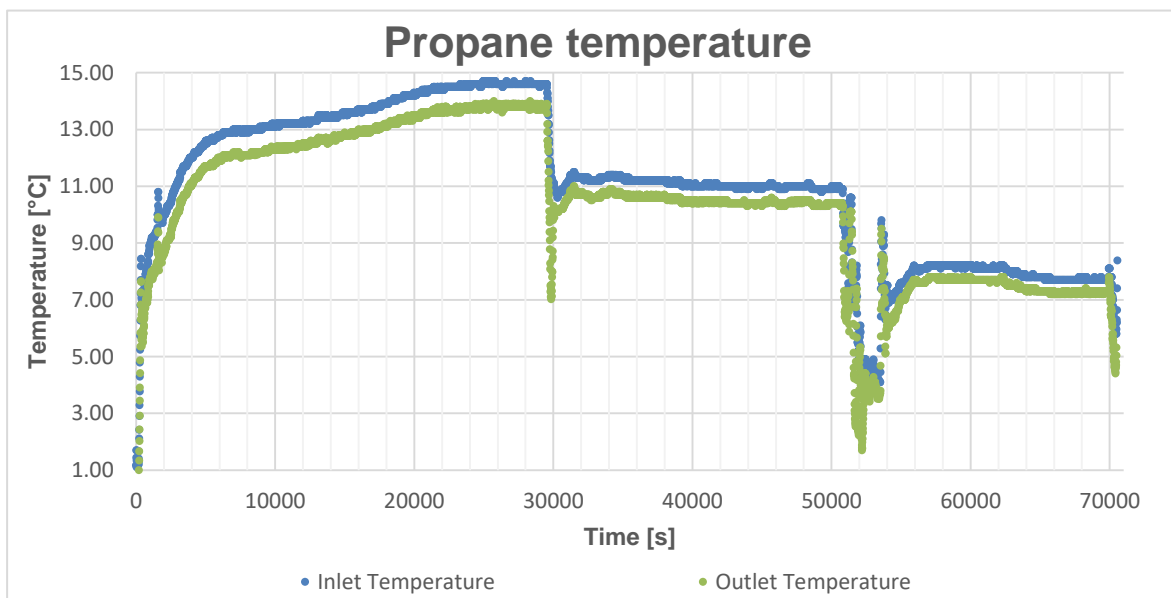


Figure 4.2 set of experimental temperature values obtained in Final Test in MoNiKa

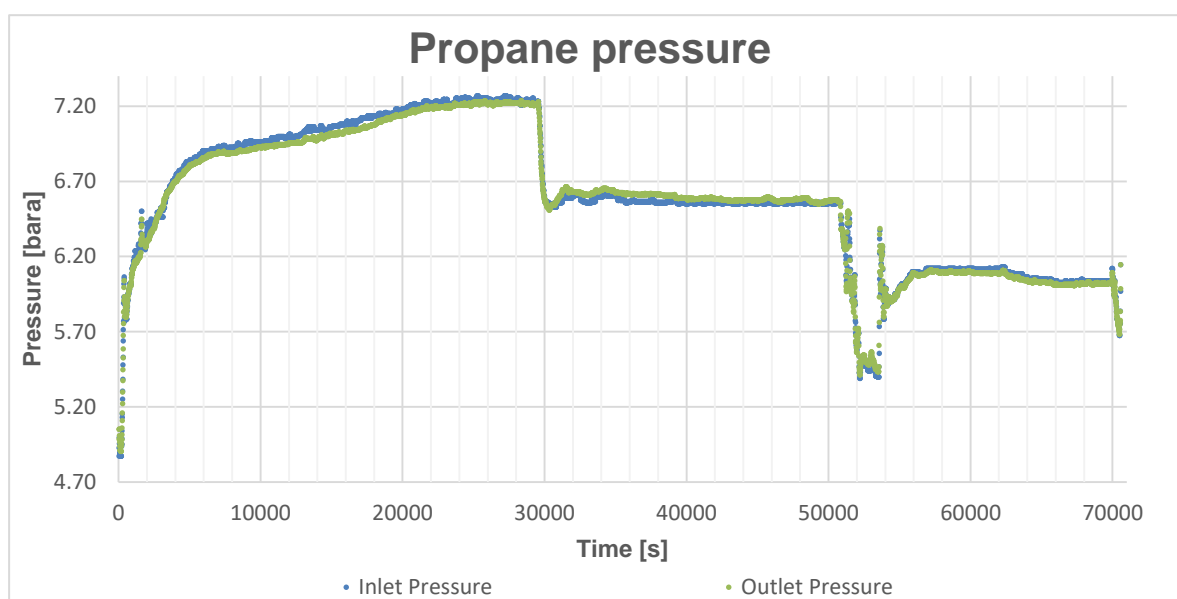


Figure 4.3 set of experimental pressure values obtained in Final Test in MoNiKa

The second transient is the change from 100% load to 70%. At simple look, this seems to be the best set of data for validation. There is an interesting undershooting in the temperature for the model to predict. The following change on load is from 70% to 50%, this set of values was discarded because there were a few problems in the control of the throttling valve that produced some instabilities not representative of the change of load in the systems, like the overshooting in the temperature and pressure in the middle of the transient because the mass flow undershoot. The final transient is at 70000 s when the cycle is shut off. This transition is smoother than the previous one and will be tested as case 2, until the velocity of the fans starts to drop. The following figure has a better display of the values of the two cases selected:

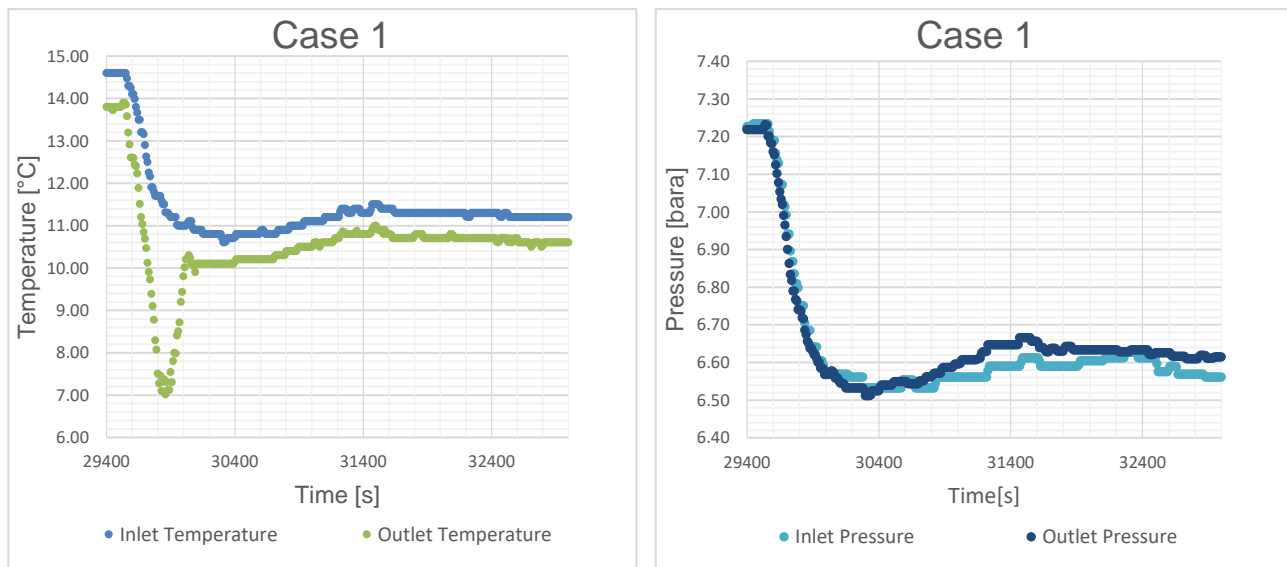


Figure 4.4 set of values for the transient case 1.

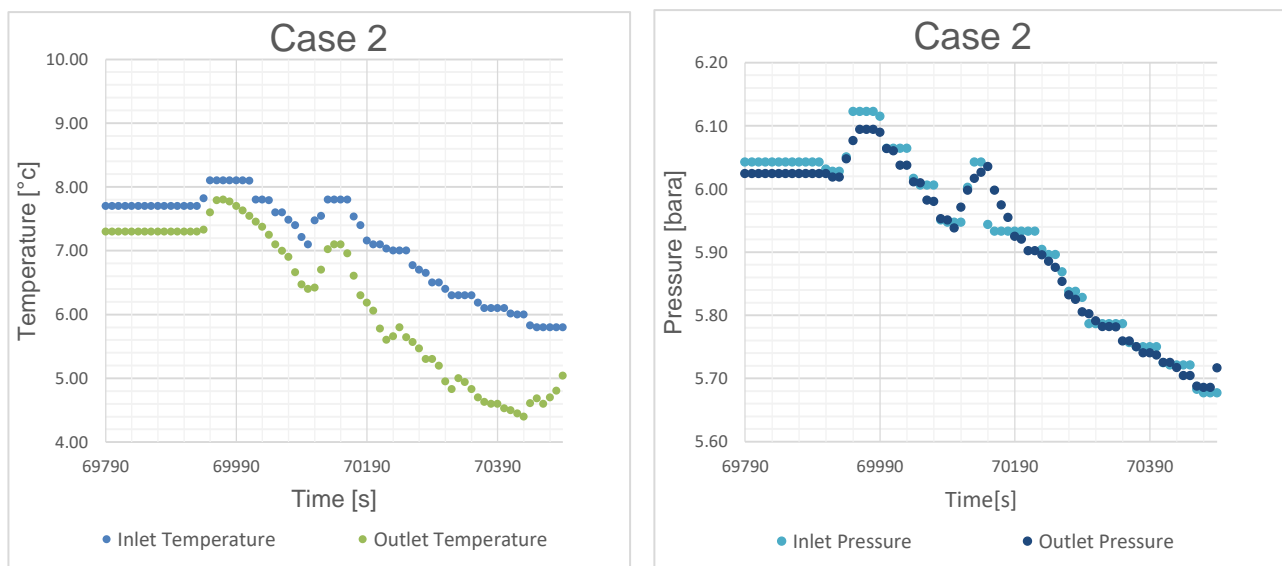


Figure 4.5 set of values for the transient case 2.

4.2 Verification

The model used in the program is a simplification version of the reality, therefore all results are affected by error in some point. In order to make a good analysis of the results it is necessary to define and calculate the errors.

In order to do a verification and check the numerical error and the convergence of the model, the definition of absolute and relative deviation is:

$$\Delta Y_a = |Y_{i-1} - Y_i| \quad (4.1)$$

$$\Delta Y_r = \frac{\varepsilon_a}{|Y_{i-1}|} \quad (4.2)$$

The smaller the value of ε_r for the evaluating of the convergence, the more accurate the model is. Subscript i corresponds to the size of the discretization that could be in time or space and subscript $i-1$ refers to a smaller size of discretization, this can be traduced as a smaller time step or a higher number of cells.

The values unknown and predicted used for this verification are the following:

- Enthalpy is the property that defines the energy balance of the system.
- Pressure is the property that defines the momentum balance of the system.
- Temperature is a basic property of the fluid measured along with the pressure.
- $\Delta h \cdot \dot{M}$ is the most significant term predicted in the energy balance.
- Pressure loss is the most significant term predicted in the momentum balance.

$\Delta h \cdot \dot{M}$ is equal to the heat exchanged in a stationary regime and, together with the pressure loss, are the values being predicted by correlations: in the first case, the correlations that confirm the global heat exchange coefficient and in the second case the correlation for the pressure loss coefficient. Keeping this in mind, is important to analyze those values to have a better understanding of the accuracy of the correlations.

The first verification was done for the number of cells. At first there were only three cells until the program could run without small errors. Then I started testing with 10 cells and real values, and some convergence error start to arise. After that I continue working with 20 cells and that was the perfect size for testing all along different kind of correlations and input conditions. The relative error between values obtain with 20 cells discretization and 40 cells discretization is small and presented in Table 4.2; for this reason the development of the program was with 20 cells. In order to save compilation and running time of the program during the analysis, a 10 cells model was used and final results were predicted with 20 cells.

ΔY_r 20/40 cells			
MoNiKa part load	100%	70%	50%
Enthalpy [%]	0.19	0.66	0.19
$\Delta h \cdot \dot{M}$ [%]	0.13	0.39	0.12
Pressure [%]	0.04	0.02	0.00
Pressure Loss [%]	3.36	3.45	2.97
Temperature [%]	0.07	0.20	0.20

Table 4.2 relative deviation between values predicted with 20 and 40 cells

The relative deviation of the pressure loss is not really small but the absolute deviation values are around of 1.3 E-4 MPa, which are negligible compared with the absolute deviation of the pressure sensor which is of 1E-2 MPa and 3E-3 MPa for the inlet and outlet respectively as shown by Table 4.1. The rest of the values of the previous table are smaller or in the same order as the relative deviation of the sensors, consequently 20 cells are used as final space discretization.

In the case of the discretization in time, the Simulink feature of an automatic time step is used. For this purpose the relative tolerance is determined to control the accuracy of integration during simulation. At each simulation step i , the solver estimates the local error e in the state j of the simulation [26]. The solver reduces the size of time step i until the error of the state satisfies:

$$|e(i,j)| \leq \max(Relative\ Tolerance * |y(i,j)|, Absolute\ Tolerance(i,j)) \quad (4.3)$$

The relative deviation for different values of Relative Tolerance were calculate until the predicted values converge. Table 4.3 displays the relative deviation between values predicted with relative tolerance of 1E-2 and 1E-3:

ΔY_r 1E-2/1E-3 relative tolerance			
MoNiKa part load	100%	70%	50%
Enthalpy [%]	0.32	0.00	0.00
$\Delta h \cdot \dot{M}$ [%]	0.21	0.00	0.00
Pressure [%]	0.00	0.02	0.00
Pressure Loss [%]	0.22	0.27	0.00
Temperature [%]	3.75	0.32	0.00

Table 4.3 relative deviation between values predicted with 1E-2 and 1E-3 of relative tolerance in time

The relative error in the case of the temperature for the 100% load is high, therefore I decided to use a relative tolerance of 1E-4, in which this value becomes zero, when compared to a value obtained with a relative tolerance of 1E-3 and so further refinement is not needed. The final relative tolerance used is 1E-3.

After this verification, I considered that the predictions of the model converged and so it was time to start analyzing and validating the equations and empirical correlations of the model.

4.3 Stationary validation

To verify the accuracy of the program in Simulink, two methods are considered: the comparison with experimental data and the comparison with data obtain with REFPROP and two independent properties measured. The data obtained by REFPROP is consider to have a good accuracy and it is already validated. The properties to be compared are the same listed in section 4.2 for verification, pressure, pressure loss, temperature, enthalpy and $\Delta h \cdot \dot{M}$. \dot{M} , the mass flow, is a constant in the model, therefore it is the same to do the comparison with or without its influence, but since this value is equal to the heat exchanged by the condenser, I think it is more representative of the system.

The absolute and relative error for the validation is defined as:

$$\varepsilon_a = |V_{measured} - V_{predicted}| \quad (4.4)$$

$$\varepsilon_r = \frac{\varepsilon_a}{|V_{measured}|} \quad (4.5)$$

4.3.1 Pressure validation

Since the pressure is measured at the inlet and outlet of the condenser, the validation will be against experimental data, also the value of the pressure loss will be indicated.

In Table 4.1 can be seen that the perceptual error of the pressure sensor at the inlet is 3 times more than the one at the outlet, subsequently is essential to remark that there is an important error in the input of the model that may affect the results. The following table presents the comparison between predicted and measured values:

Pressure			
MoNiKa part load	100%	70%	50%
Predicted [Mpa]	0.716	0.651	0.597
Measured [Mpa]	0.722	0.658	0.602
Sensor absolute deviation [Mpa]	± 0.003	± 0.003	± 0.003
Absolute error [Mpa]	0.006	0.007	0.005
Relative error [%]	0.83	1.06	0.83

Pressure Loss			
MoNiKa part load	100%	70%	50%
Predicted [Mpa]	0.00812	0.00515	0.00328
Measured [Mpa]	-0.002	0.0018	0.0056
Sensor absolute deviation [Mpa]	± 0.013	± 0.013	± 0.013
Absolute error [Mpa]	0.01012	0.00335	0.00232
Relative error [%]	506.00	186.11	41.43

Table 4.4 pressure and pressure loss validation data

All these predicted data were acquired with the correlations presented in section 2.5, no other correlation for the pressure was tested. The relative error of the pressure values is no more than 1.1%. With this in mind it is possible to say that the model cannot be far away from the reality, or at least is in the same order of magnitude. The problem with these values is that the pressure loss, both measured and predicted, are really small compared with the pressure values, by around 1 or 2 orders. Consequently, the pressure loss values are smaller than the sensors deviation and so there is no certainty on the validation of the pressure values, since the main effect to predict the pressure is the pressure loss.

The same goes for the values presented for the pressure loss. The relative errors are really high but comparing the absolute error with the sensors deviation, it is smaller, and so there is no certainty on the validation either. With the first measured values, this scenery was already somehow predicted. The average pressure loss presented is negative and this is not expected in a stationary regime, for the fluid to lose heat and to gain pressure with a constant mass flow.

The model consist on the simulation of only one tube, under the assumption that the mass flow, is distributed equally in all the tubes. This assumption, neglects the difference in hydrostatic pressure between tubes. This neglected pressure, could be one of the reasons why the pressure is being under-predicted.

Another verification was made: the fluid was consider all the way as a liquid phase and as a gas phase and the pressure loss for the single phases was predicted with the correlation presented in section 2.5. The values obtained for the mixture presented in the previous table were between this two limit values.

4.3.2 Temperature and enthalpy validation

The other value that is predicted by solving the balances is the enthalpy, therefore is significant to make an analysis about this value as well. The validation is done by comparing the value predicted and the one calculate by REFPROP with the pressure and temperature measured. This last value is expressed with the error of both sensors and the REFPROP data. Another value to contemplate for the analysis is $\Delta h \cdot \dot{M}$ which is equal to the heat exchanged in the stationary points. Another value to compare for the validation is the temperature, in this case the comparison is directly with measured data.

The measured values of the enthalpy shows that the propane is leaving the condenser a little subcooled but really close to the saturation when it is compared with the saturated enthalpy value for the respective pressure. This is an important fact to take in account when analyzing the temperature data. In case that the enthalpy is over-predicted, which means that the condenser exchanges less heat than in the reality, the value of the temperature will have a limit in the saturate state defined by the pressure. This limit in the prediction of the temperature is really close to the real value since the fluid is just a little subcooled. This means that, in this case if the pressure is well predicted, the temperature will not show any signs of error in the model, and that it is why is important to also compare the enthalpy values.

In other hand, the prediction could be more subcooled than the reality, this scenario has also a limit, which is the ambient temperature. The best ideal scenario is that the propane temperature reaches a value around the average temperature of the air and this makes a small window for error when the prediction is overcooled. In the program, there is a warning message which indicates that the temperature of the air must be lower than the one of the propane. This lower limit works for the enthalpy and temperature of the propane, which could not get colder than the average temperature of the air.

The limits for the enthalpy and the temperature are displayed in Table 4.5. The values of the temperature are expressed in the relative scale of Celsius because it is better for grasping the dimension of the limits for the ambient temperatures. When expressed in the absolute scale and the relative error is calculated, the range of possible temperatures turns to be really small.

Limits for the temperature range			
MoNiKa part load	100%	70%	50%
Measured pressure [Mpa]	0.722	0.658	0.602
Measured temperature [°C]	13.8	10.4	7.2
Upper limit, Saturated temperature [°C]	14.5	11.2	8.0
Lower limit, average air temperature [°C]	3.89	2.89	1.7

Limit for the enthalpy range			
MoNiKa part load	100%	70%	50%
Measured pressure [Mpa]	0.722	0.658	0.602
Measured enthalpy (REFPROP) [kJ/kg]	235	226	218
Lower limit, Enthalpy at air temperature [kJ/kg]	209.9	207.3	204.3
Saturated Liquid enthalpy [kJ/kg]	237.2	228.4	220.4

Table 4.5 temperature and enthalpy limits for the scenario of study

The saturated enthalpy is displayed to give an idea of the proximity of the outlet enthalpy values to the liquid saturation point.

We have to keep in mind, of course, that these specific limits are for the data gathered in this points, and they change with the ambient parameters, not only with air temperature but also with pressure, which varies with the ambient temperature. At the exit of the condenser, an accumulation tank of propane is located. This tank is full with liquid and gas propane in a saturated state. The state of the tank is defined by the properties of the propane inside it like pressure, temperature and volume of gas, but also by the ambient temperature. Therefore the effects of the ambient temperature are twofold, to set the lower temperature of the cycle and thus the pressure for that saturation state and to influence the properties inside the tank of propane which is also affecting the properties inside the condenser.

All the physical limitations on the model were presented, so that the values predicted, presented in Table 4.6, can be better analysed. At first I tried several correlations for the outer and inner heat transfer coefficient. If the values of the enthalpy reached the lower limit and if there is no warning or a manual check of the temperature of the propane and the air, the program can simulate that the air release heat into the propane in some cells, even if the global heat transfer coefficient is not well approximated. Of course this problem was solved not only with a warning message. Also there is not heat exchange, when the temperature of the propane is equal or below the average air temperature. After that, I tried to get a better approximation so that the value of the enthalpy would not be at the lower limit, because that also means that the prediction of heat exchanged in the condenser is bounded only to the variation of the air temperature. Then the sensibility on the other variables will be practically lost. This effect is well noticed in the transient predictions, where, if the simulation reaches the enthalpy lower limit, the temperature predicted copy the form of the air temperature and does not reassemble the form of the measured values.

The relative error for the predictions of the enthalpy is inside of a 10% deviation. The same goes for the enthalpy difference and in the temperature case is inside the 5% deviation. For this last value, it is better to take a look at the absolute error, where the values are around the 5 K in a possible range of temperatures between 10 K or 8 K, depending on the part load.

Enthalpy			
MoNiKa part load	100%	70%	50%
Predicted [kJ/kg]	217.3	212.9	209
Measured (REFPROP) [kJ/kg]	235	226	218
Sensor and REFPROP absolute deviation [kJ/kg]	± 0.5	± 0.5	± 0.5
Absolute deviation [kJ/kg]	17.7	13.1	9
Relative Deviation [%]	7.53	5.80	4.13

$\Delta h \cdot \dot{M}$			
MoNiKa part load	100%	70%	50%
Predicted [kW]	-975	-696.5	-495.9
Measured (REFPROP) [kW]	-922	-670	-482
Sensor and REFPROP absolute deviation [kW]	± 10	± 7	± 5
Absolute error [kW]	53	26.5	13.9
Relative error [%]	5.75	3.96	2.88

Temperature			
MoNiKa part load	100%	70%	50%
Predicted [K]	280.5	278.8	277.2
Measured [K]	287.0	283.5	280.4
Sensor absolute deviation [°C]	± 0.18	± 0.18	± 0.18
Absolute error [K]	6.45	4.80	3.23
Relative error [%]	2.25	1.69	1.15

Table 4.6 Temperature, enthalpy and enthalpy difference validation data

4.4 Transient validation

With the steady-state validation for three part load conditions and having two cases already selected for the transient validation, the next step was to prepare all transient data in an excel sheet, and to feed it as an input to the Simulink program. The first value to be presented, is the predicted pressure, together with the measured one at the outlet and inlet of the condenser. As shown in Figure 4.6, the predicted outlet pressure has a similar shape as the inlet pressure, but with an offset given by the pressure loss. The values of the measured outlet pressure sometimes exceed the inlet values, which can be explained by, the missing hydrostatic pressure and by the deviation in the sensor. There is not a lot to analyze in this case because, as was presented in the previous subsection, the relative error of the pressure is small, since the pressure loss in the condenser is really small compared to the absolute pressure values, and too small for the accuracy of the sensors installed.

The second set of data presented is the one referred to the enthalpy. The process for obtaining the enthalpies presented as “estimated with REFPROP” were already explained in this section. As can be seen in Figure 4.7, the enthalpy at the condenser outlet is under-predicted, meaning that the prediction is more subcooled than the enthalpy, which REFPROP estimates based on measured temperature and pressure at the condenser outlet. The predicted outlet enthalpy stays fairly constant, because the predicted temperature is close to the ambient temperature, and thus the outlet enthalpy is really close to the lower limit, discussed in the previous section. There is a small valley in the predicted outlet enthalpy, before 500 s. It is almost imperceptible in the graphic, but it is located where the estimated with REFPROP outlet enthalpy has its minimum.



Figure 4.6 Transient pressure data for case 1

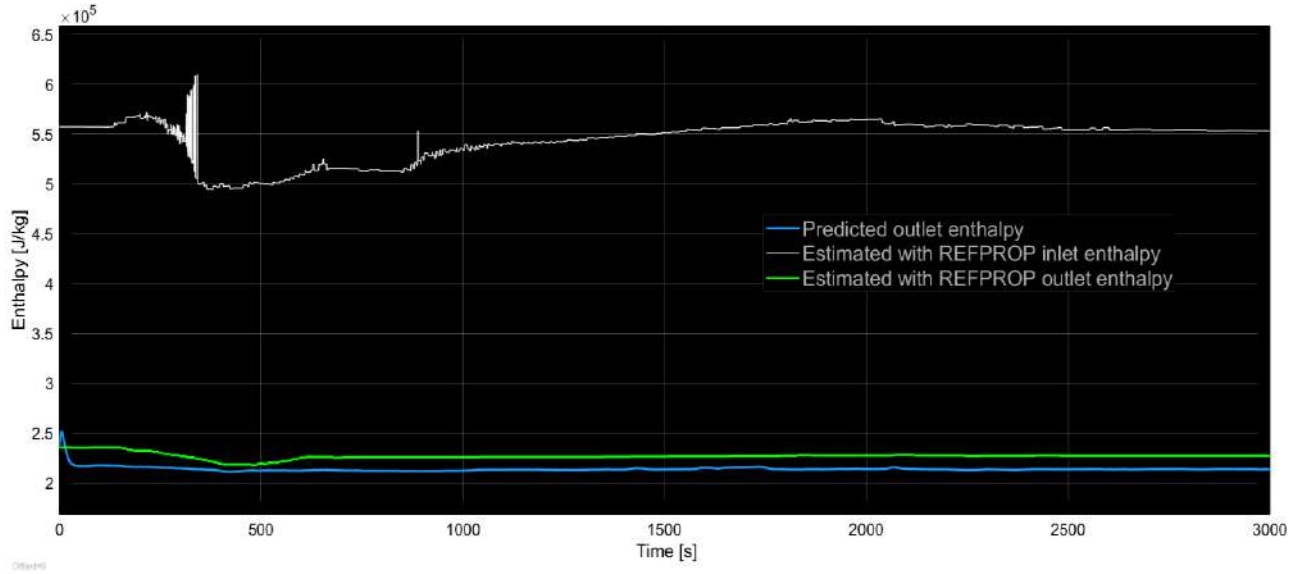


Figure 4.7 Transient enthalpy data for case 1

The abrupt change of the inlet enthalpy is explained by the change in the mass flow, which is displayed in Figure 4.8. Measured and predicted mass flow are identical by definition. For changes of the operational points during the test, first the mass flow of the geothermal water was adjusted, which is the heat source, then the mass flow of the propane, and then the operational point of the pumps. The control of the throttling valve was made manually and without any feedback control method, which explains several step changes until the desired point was reached. The reason of the noise on the signal is the Coriolis mass flow sensor, which is located after the piston pump. The frequency of the noise should match to the one of the strokes of the pump.

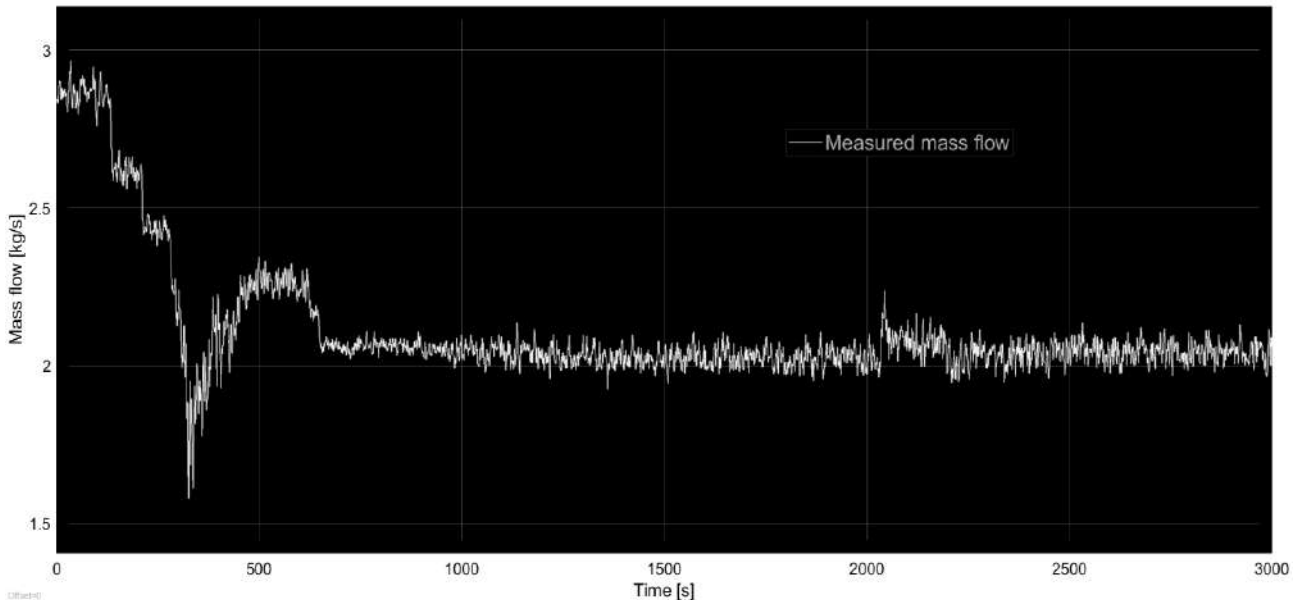


Figure 4.8 Transient mass flow data for case 1

For the entire test period, the frequency speed of the fan was set to the maximum and so the value of the air mass flux was expected to be constant. The only way to check the air mass flux was to check the line frequency of the fans which was stable in the case 1.

In Figure 4.9 the temperature data are presented. The condenser inlet temperature is identical with the measured one by definition. The predicted outlet temperature is lower than the measured one by 4 to 6 °C. In fact, it is rather close to the ambient air temperature. This results agrees with the comparison of outlet enthalpies. Obviously, heat transfer in the condenser is somewhat overpredicted.

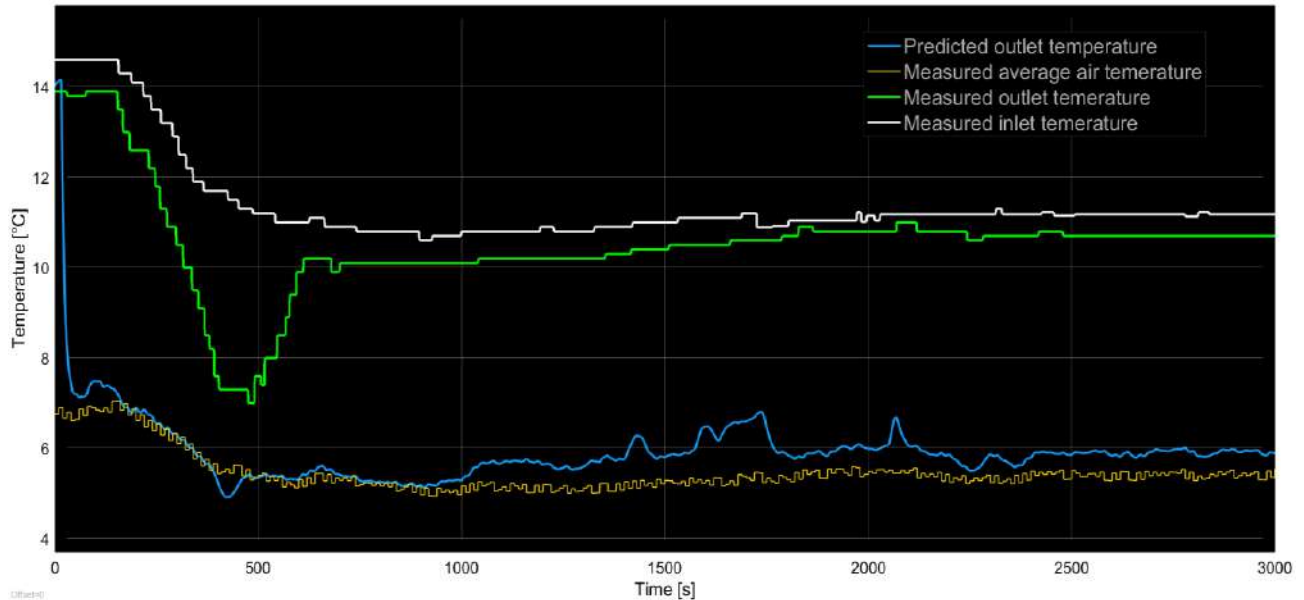


Figure 4.9 Transient temperature data for case 1

The relative error, as was calculated for the stationary points in the previous section in equation (4.5), is presented for the predicted values for each time step in Figure 4.10. The enthalpy and temperature error shows a minimum just before the 500 s because the predicted enthalpy is quite constant and there is a minimum in the outlet enthalpy estimated with REFPROP as has been displayed already in Figure 4.7.

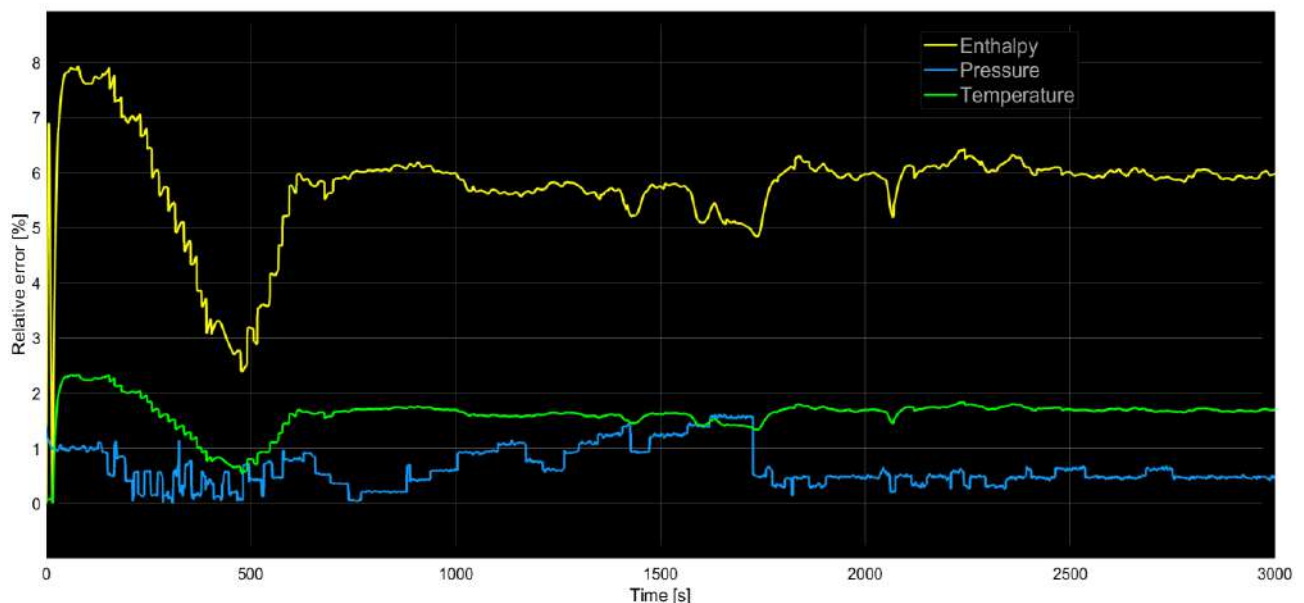


Figure 4.10 Relative error for the transient data for case 1

For better comparison with measured temperatures, I corrected the overall heat transfer coefficient of the condenser by a constant factor. However this does not produce a linear effect in the heat transferred, because, if the value of k is reduced by a constant in each cell, the heat transferred in the cells will change and also the distribution of the quality and pressure inside the tubes. Consequently, an additional effect in the value of k of each independent cell will appear, because, the heat transfer coefficient on the propane side depends on the quality and the pressure of the condensing propane.

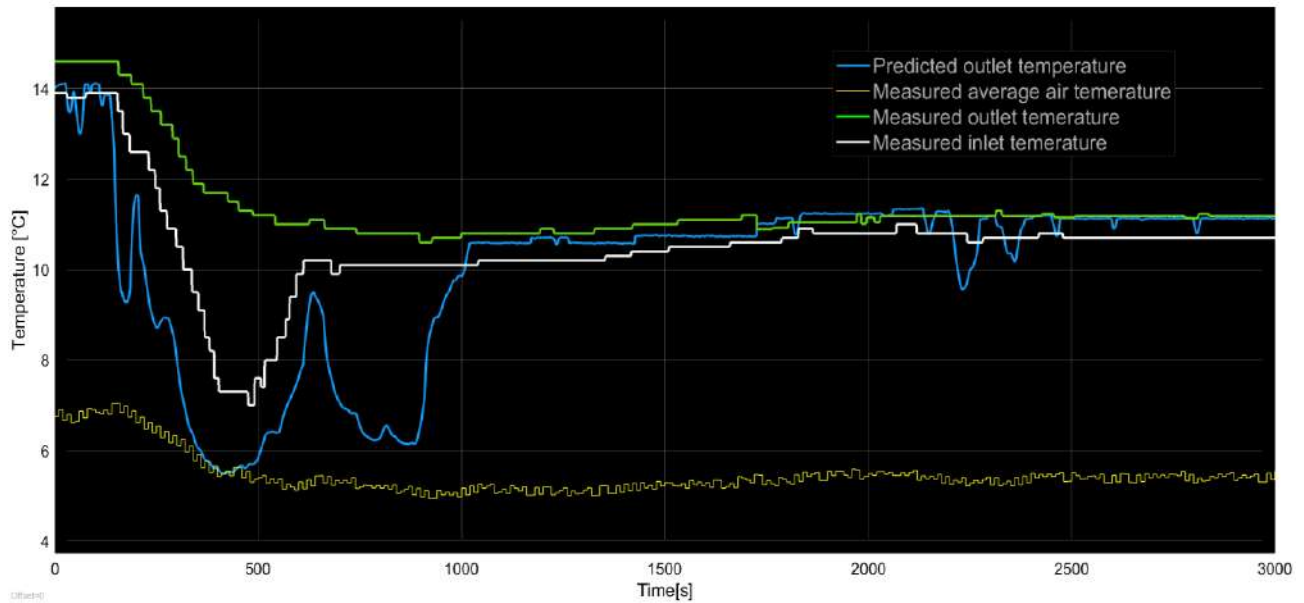


Figure 4.11 Transient temperature data if k predicted is corrected by a constant factor 0.9 for case 1

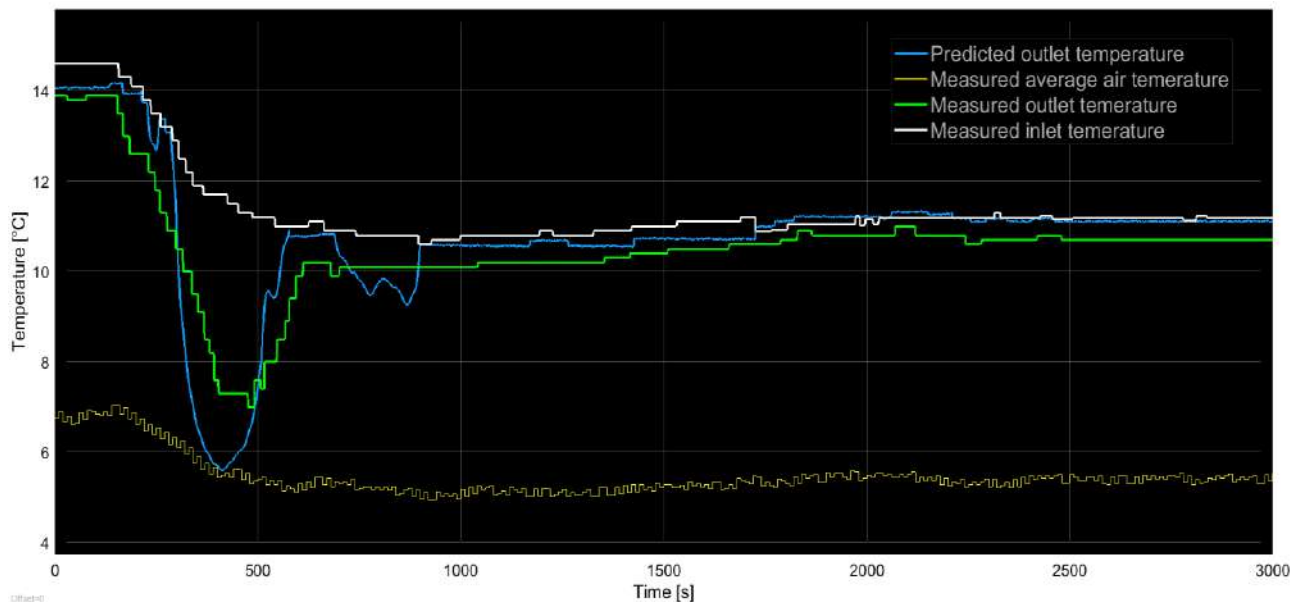


Figure 4.12 Transient temperature data where k predicted is affected by 0.85 constant for case 1

Figure 4.11 shows the effect of a constant correction factor of 0.9 multiplied with the overall heat transfer coefficient k . The local minimum at 400 to 500 s is now well reproduced with some local over

and under shootings. A second minimum at 700 to 900 s, however, has not been measured as predicted. After 1000 s the signal appears to be close to the saturation temperature as measured. In another test, the correction factor was chosen to be 0.85. We see in Figure 4.12 that the shape of the predicted curve has a little more resemblance to the one measured at the exit, but also great part of the signal is really close to the inlet temperature which is the saturation one and so this means that the limit was reached.

The absence of the thermal inertia inherent to the mass of the structure of the condenser in the energy balance, which is not taken into account in the present model, could be an explanation for the local high amplitudes of fluctuations of the temperature in some regions. If the mass of the tubes is added to the energy balance, a smother curve might be predicted.

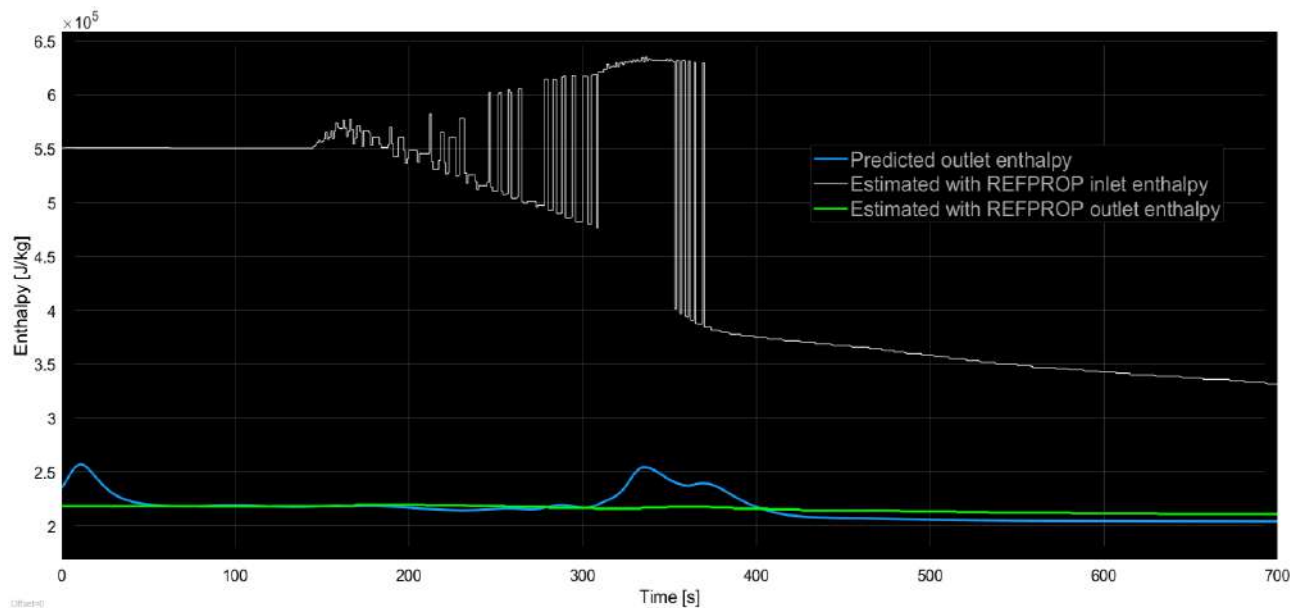


Figure 4.13 Transient enthalpy data for case 2

A similar validation analysis of the case 2 was not possible. The main reason is displayed in Figure 4.13, where it can be seen that values of the enthalpy at the inlet have high oscillations. They went from 630 kJ/kg to 370 kJ/kg approximately. These oscillations are not real. This effect is given instead by the reduction of the measured temperature in the point 3, before the throttling valve, from which the enthalpy at the condenser inlet is approximated. In this specific case, facility was shut down, this means that the temperature of the propane started to decrease around 200 s. When the temperature is under the critical one, the point 3 starts to be inside the saturation zone or at least close to the saturation line. Pressure and temperature do not define the enthalpy anymore then. A minimal deviation of inlet values, however can result in a value of subcooled or overheated enthalpy at the outlet. In the saturation zone, pressure and temperature are linked and information of the quality of the fluid is missing. The oscillations, which we see in Fig. 4.13 are thus simply the consequences of small fluctuations in temperature, for which REFPROP is giving either saturated liquid or saturated vapor enthalpies. Therefore the analysis of the second case was done but discarded because of the instability of the enthalpy approximation at the inlet.

5 Summary and Conclusions

The objective of this master thesis was to develop a transient model suitable for the condenser already installed in MoNiKa. The program is capable of working for different values of geometries, inside the correlations limits, but always maintaining the global premise of a condenser with horizontal pipes and plain fins refrigerated by air. The primary fluid can be changed to one of the many fluids tested for the correlation used for the inner heat transfer coefficient and has to be on the REFPROP database.

The model presented in the study contains some simplification that resulted in a model capable of a good prediction of the MoNiKa condenser in regular operation status of the cycle and of being developed and tested in the time lapse limit for a master thesis. It is a good ground model, which can be upgraded by adding consideration to the different simplifications that has been done and so fulfill a more complete model, which can predict with more accuracy and in non-common operational points. The first upgrade I would suggest is to include the equations for humid air. This will change the performance of the condenser, but for that, some experimental data will be needed to validate. The second is to include the thermal inertia of the mass of the condenser structure. It will not change the prediction of the stationary points, but there is the possibility to change the behavior of the transients. It should smoothen the predicted signals in the heat transfer part of the model. The third upgrade is to be discussed, but could be the consideration of the quick changes in densities, mass and pressure. In case of doing a study fast transients of the cycle, different sensors must be installed and specific test must be performed. Moreover, a simulation of the entire ORC cycle will provide better inlet and outlet conditions of the condenser.

The program runs in a very reasonable time, but still there is some window to improve the efficiency of the program structure, keeping in mind that, before this work, I had no experience working with Simulink. I can say that the idea and following application of the use of two phase tables was really good and a big help for the small simulation periods. It is very practical to set the range of pressure and internal energy that the simulation will run, and then work with the lookup table block, which has different interpolation method and thus produce really small errors. At first, the idea of calling the REFPROP for each time step, in each cell and for each property really worries me because of the computing time, and this proved to be a really good solution and improvement. However, there is an unpractical point for this feature, and that is that the amount of properties is limited to basic ones and already set by the function on Matlab. It has all the properties that I needed for my simulation except for the surface tension, which is constant for the saturation zone and has little and linear variability for the range of study. Also the program is not very sensitive to this value.

The data obtained for validation was limited, and it would be good to test the model in another different scenarios with different settings of the plant. An important part of the simulation is the approximation of the enthalpy at the inlet of the condenser by the assumption of an isentropic throttling valve, this means that, when the cycle runs with a turbine, it is important to have an accurate curve of the isentropic efficiency to incur in the minimal possible error for the prediction of the input data for enthalpy. More data with different ambient condition would be really interesting to analyze and to conclude how it affects the model. As it is known, the ambient temperature set the minimal

temperature in the cycle and the ideal maximum efficiency, it also fixes the pressure on the condenser and therefore the range of values where the predictions can be obtained.

In the case of the validation of the pressure loss, sensors with better resolution are needed to be able to make a conclusive study. Instead of installing new sensors in the cycle, it may be easier to make external test with a similar tube and different propane mass flows to specify a more accurate pressure loss. The prediction of the pressure is already inside the 2% of deviation, but this can be improved, always keeping in mind that as long as the pressure is relative well predicted, the temperatures have a little range of possibilities limited by the air temperature and the saturation temperature for that pressure value. If a better prediction of pressure is wanted, the sensor at the inlet with 1.38% of relative deviation needs to be upgraded to be able to do a conclusive validation of those values. The predicted values for the stationary and transient validation presented were inside a deviation of 8% for the enthalpy and 2% for the pressure. In order to conclude a correction function to reach a more accurate prediction, more time and wider set of data is needed so that the function can be applied to different boundary conditions. The relative deviation for the predicted values of the temperature is also good, but the absolute deviation value in the relative scale of Celsius can be considered high. To be able to improve this value, the enthalpy prediction must be enhanced.

The period of selection for the correlation used in the program was important, since the difference in the predicted values between correlations was considerable. Is not easy to find a correlation for the air side that meets all the conditions for the condenser already installed, and the one used it is suggested by the author that can be slightly modified inside a range to made certain effects of the geometry more or less significant. There are many options for empirical correlations, but just a few meet the requirements. This also happens with correlations for the inner heat transfer coefficient, were only a few were tested for propane, the different values of Reynolds and Prandtl number must be on the range specified by the author and the type and regime of condensation have to be taken in account.

The model created in Simulink can be enclosed in a block with only 3 inlets and 3 outlets (pressure, enthalpy and mass flow) for the propane and the inlet and outlet temperature of the air. This kind of block, has the potential of being part of a general model created to simulate the entire MoNiKa plant.

6 References

- [1] A. E. Bergles, J. G. Colier, J. M. Delhay, G. F. Hewitt und F. Mayinger. 1981. *Two-phase flow and heat transfer in the power and process industries*. Hemisphere Publishing Corp., Washington – New York – London.
- [2] Akers, W.W., H.A. Deans, and O.K. Crosser. 1959. Condensing heat transfer within horizontal tubes. *Chemical Engineering Progress Symposium Series* 59, 171–176.
- [3] Kuan-Yu C. Chi-Chuan Wang. 2000. Heat transfer and friction characteristics of plain fin and tube heat exchangers, part I: new experimental data. *International Journal of Heat and Mass Transfer* 43, 2681–2691.
- [4] A. P. Colburn. 1933. A Method of Correlating Forced Convection Heat Transfer Data and a Comparison with Fluid Friction. *Trans. AIChE* 29, 174–210.
- [5] J. El Hajal, J.R Thome, and A. Cavallini. 2003. Condensation in horizontal tubes, part 1: two-phase flow pattern map. *International Journal of Heat and Mass Transfer* 46, 18, 3349–3363.
- [6] L. FRIEDEL. 1978. Druckabfall bei der Strömung von Gas/Dampf-Flüssigkeitsgemischen in Rohren. *Chemie Ingenieur Technik* 50, 167–180.
- [7] L. FRIEDEL. 1979. Improved friction pressure drop correlations for horizontal and vertical pipe flow. *3R Int* 18, 485–492.
- [8] Volker Gnielinski. 1975. Neue Gleichungen für den Wärme- und den Stoffübergang in turbulent durchströmten Rohren und Kanälen. *Forsch. Ing.-Wes* 41, 8–16.
- [9] Gray, D. L., and Webb, R. L. 1986. Heat Transfer and Friction Correlations for Plate Finned-Tube Heat Exchangers Having Plain Fins. *Heat Transfer* 6, 2745–2750.
- [10] Incropera, Frank P. and DeWitt, David P. 2002. *Fundamentals of Heat and Mass Transfer (5th ed.)*. Hoboken: Wiley.
- [11] P. K. KONAKOV. 1954. Eine neue Formel für den Reibungskoeffizienten glatter Rohre. *Bericht der Akademie der Wissenschaften der UDSSR* 51, 503–506.
- [12] KTK Kühlturm Technologie GmbH. 2015. Process and plant description MoNiKa Condenser. Technical Documentation.
- [13] F. C. McQuiston. 1978. Correlations of Heat, Mass and Momentum Transport Coefficients for Plate-Fin-Tube Heat Transfer Surfaces with Staggered Tubes. *ASHRAE Trans* 84, 294–309.
- [14] N. Kayansayan. 1993. Heat Transfer Characterization of Flat Plain Fins and Round Tube Heat Exchangers. *Experimental Thermal and Fluid Science* 6, 263–272.
- [15] J. Nikuradse. 1933. Strömungsgesetze in rauen Rohren. *Forschung Auf dem Gebiete des Ingenieurwesens. NACA Technical Memorandum* 1292.

- [16] NIST. 2018. *REFPROP. Standard Reference Database 23: Reference Fluid Thermodynamic and Transport Properties*. NIST, Bd. 9. Gaithersburg, Colorado, USA: National Institute of Standards and Technology.
- [17] NIST. 2018. *REFPROP Documentation. General information*.
- [18] Prof. Dr. Thomas Schulenberg. *Two Phase Flow Fluids and Zweiphasenströmung mit Wärmeübertragung lecture material*.
- [19] Prof. Dr. Thomas Schulenberg. 2016. *OTEST. MATLAB Code System Solving the One-Dimensional Transport Equations for Single and Two-Phase Flow in Pipes. Unpublished*.
- [20] Ronald DiPippo. 2008. *Geothermal Power Plants: Principles, Applications, Case Studies and Environmental Impact*. ELSEVIER.
- [21] M. M. Shah. 1979. A general correlation for heat transfer during film condensation in pipes. *International Journal of Heat and Mass Transfer* 22, 547–556.
- [22] M. M. Shah. 2009. An improved and extended general correlation for heat transfer during condensation in plain tubes. *HVAC&R Research* 15(5), 889–913.
- [23] Th.E. Schmidt. 1949. Heat transfer calculations for extended surfaces. *Refrigerating Engineering*, 351–357.
- [24] The MathWorks, Inc. 2019. *MATLAB*.
- [25] The MathWorks, Inc. 2019. *Simmulink*.
- [26] The MathWorks, Inc. 2019. *Simulink Documentation*.
- [27] 2010. *VDI Heat Atlas*. Springer Berlin Heidelberg.
- [28] Christian Vetter, Hans-Joachim Wiemer, and Dietmar Kuhn. 2013. Comparison of sub- and supercritical Organic Rankine Cycles for power generation from low-temperature/low-enthalpy geothermal wells, considering specific net power output and efficiency. *Applied Thermal Engineering* 51, 1-2, 871–879.
- [29] Wentech. 2015. *Technical documentation Rotor WO 2475-3-(14) AS/SG-4. Manufacturer document*. Retrieved from.
- [30] E. A. Z. Rouhani. 1970. Calculation of void volume fraction in the subcooled and quality boiling regions. *Int. J. Heat Mass Transfer* 13, 383–393.

7 Appendix

7.1 List of tables

Table 3.1 Two phase fluid tables properties.....	25
Table 4.1 Stationary points and values for validation	34
Table 4.2 relative deviation between values predicted with 20 and 40 cells	38
Table 4.3 relative deviation between values predicted with 1E-2 and 1E-3 of relative tolerance in time.....	38
Table 4.4 pressure and pressure loss validation data	39
Table 4.5 temperature and enthalpy limits for the scenario of study.....	41
Table 4.6 Temperature, enthalpy and enthalpy difference validation data.....	42

7.2 List of figures

Figure 2.1 Diagram of the Rankine Cycle.....	3
Figure 2.2 T-S Diagram of MoNiKa ORC at full load	3
Figure 2.3 MoNiKa condensers layout [12]	4
Figure 2.4 Condenser heat exchange module [12].....	5
Figure 2.5 Air flow path in the condenser [12]	5
Figure 2.6 Fin stack and tube bundle arrangement	5
Figure 2.7 geometry and arrangement of the tube bundle in a fin	17
Figure 3.1 model hierarchy	23
Figure 3.2 difference in phase diagrams using internal energy an normalized internal energy [26] .	26
Figure 3.3 Flow diagram of the program	27
Figure 3.4 Cell Subsystem	28
Figure 3.5 Energy balance subsystem diagram	30
Figure 4.1 T-S diagram of MoNiKa, in red condensation zone of the cycle is marked	33
Figure 4.2 set of experimental temperature values obtained in Final Test in MoNika	35
Figure 4.3 set of experimental pressure values obtained in Final Test in MoNika	35
Figure 4.4 set of values for the transient case 1.....	36
Figure 4.5 set of values for the transient case 2.....	36
Figure 4.6 Transient pressure data for case 1.....	43
Figure 4.7 Transient enthalpy data for case 1	44
Figure 4.8 Transient mass flow data for case 1.....	44
Figure 4.9 Transient temperature data for case 1	45
Figure 4.10 Relative error for the transient data for case 1	45
Figure 4.11 Transient temperature data where k predicted is affected by 0.9 constant for case 1...	46
Figure 4.12 Transient temperature data where k predicted is affected by 0.85 constant for case 1.	46
Figure 4.13 Transient enthalpy data for case 2	47